4-D flight trajectory tracking: a receding horizon approach integrating feedback linearization and scenario optimization

Luca Deori, Simone Garatti, *Member, IEEE,* Maria Prandini, *Senior Member, IEEE*

***Abstract*—This paper proposes a control strategy to steer an aircraft along a given reference 4-D trajectory. The aircraft has a nonlinear dynamics and is subject to constraints related to its maneuverability and to passengers comfort. Feedback linearization of the aircraft dynamics and convex relaxation of the constraints allow for a reformulation of the trajectory tracking problem that is suitable for a receding horizon implementation. Uncertainty is affecting the aircraft motion, mainly through wind, which is described as a Gaussian random field and approximated on-the-fly by a local autoregressive model. The adoption of a scenario-based minimization of the tracking error introduced by the stochastic wind disturbance preserves the problem convexity and allows to obtain a program that can be solved with limited computational effort. The wind model update jointly with the re-computation of the control action at each time step allow to account for the spatial variability of the random field and to obtain recursive feasibility of the receding horizon solution.**

***Index Terms*—Flight control; air traffic management; trajectory tracking; feedback linearization; stochastic optimization.**

I. Introduction

Air traffic is increasing rapidly, and this growth is becoming more and more unsustainable for the current rigidly structured air traffic management system, where aircraft are forced to fly along predefined routes. New concepts for managing air traffic are needed to exploit more efficiently the airspace capacity and to avoid route congestion and delays. A possible solution that has been proposed in the literature rests on the concept of 4-Dimensional (4-D) trajectories and Target Windows (TWs), [1], [2]. TWs represent constraints on the 4-D aircraft trajectories and should allow for a more efficient use of the airspace, enhancing predictability of the aircraft trajectories and improving safety. In the CATS [1] project, TWs are viewed as a key enabler of new air traffic management systems involving all different actors (airlines, airports, air navigation service providers) in the management process.
TWs impose constraints on the aircraft motion in the time-space domain, in that the aircraft is required to pass through certain sections of the airspace within some pre-specified time frames. Additionally to the TWs, physical limitations on speed and acceleration, as well as constraints related to passengers comfort must be accounted for when controlling the 4-D motion of an aircraft. The control strategy should also be robust with respect to uncertainty and, in particular, the presence of wind, [3], [4], [5], [6], [7].

The goal of this paper is developing a control strategy that is able to steer the aircraft along a reference 4-D trajectory, robustly with respect to the possible wind disturbance realizations, while accounting for the aircraft physical limitations and for comfort and safety requirements. Aircraft motion control is addressed also in [8], [9], [10], where the presence of constraints is only partially accounted for. As for the TW specifications, we assume that the reference 4-D trajectory has been designed so as to be compatible with both the aircraft motion capabilities and the TWs, i.e., if it were initialized along this trajectory and there were no uncertainty affecting its motion, then, the aircraft could perfectly track it and meet the TWs constraints (see [11] for a method to design trajectories that complies with these requirements). Note that the trajectory is composed by a path and a time law, and tracking it requires that the aircraft is steered so as to be at the proper position, at a proper timing. Hence, by keeping the aircraft as close as possible to the reference trajectory, TW specifications are satisfied also by the actual aircraft trajectory, compatibly with the effect of the wind disturbance.

We adopt a discrete time model of the aircraft motion and a receding horizon strategy that involves minimizing at each sample time t_k a suitably defined finite-horizon cost subject to appropriate constraints so as to enforce trajectory tracking and the satisfaction of the aircraft physical limitations and passenger comfort requirements. The so obtained control action is applied at time t_k only, and the optimization process is repeated at every sample time over a receding horizon.
When formulating the finite horizon constrained optimization problem, a key issue for computational and solvability reasons is that of achieving convexity. Given that the model of the aircraft dynamics is nonlinear, we then apply feedback linearization so as to eventually globally linearize it. Yet, the constraints on the aircraft physical limitations and passenger comfort rewritten with respect to the new state and input variables of the feedback-linearized model result to be non-convex. Hence, a major effort is put in reformulating these constraints as convex constraints, introducing some relaxation, but just when needed. Such relaxations are appropriately designed so as to guarantee that the original constraints are satisfied at least for the first time instant of the current finite horizon. This way, the actually implemented receding horizon controller is guaranteed to satisfy the original constraints at

Luca Deori, Simone Garatti, Maria Prandini are with Dipartimento di Elettronica, Informazione e Bioingegneria, Politecnico di Milano, via Ponzio 34/5 20133 Milano, Italy. {luca.deori, simone.garatti, maria.prandini}@polimi.it

This work is partially supported by the European Commission under the project UnCoVerCPS with grant number 643921.

all time instants. For a different nonlinear receding horizon approach that does not resort to feedback linearization see [12].

The idea of using feedback linearization followed by a convexification of the constraints is not new as it has been adopted in [13], [14], [15], while [16] discusses the problem from a general perspective. The challenge, however, is then to solve a non-trivial global feedback linearization problem and to develop an ad-hoc method for the convexification of the constraints, a problem that still lacks a general solution.

To pursue the objective of tracking the reference trajectory, reference tracking errors are considered and their minimization is enforced within the finite horizon optimization problem. The tracking errors however depend on the wind disturbance, which makes the problem challenging because: (i) the wind disturbance depends nonlinearly on the aircraft position [17], [18], [10], and (ii) the wind disturbance is stochastic and has unbounded support. In this paper, the former issue is addressed by replacing the original wind disturbance model with a local approximation around the aircraft current position, which is accurate in the region of the airspace that the aircraft will be flying into along the look-ahead time horizon. As for the second issue, we opted for the minimization of the worst-case trajectory tracking errors over all possible wind disturbance realizations except for a set of user-chosen probability ϵ, resulting in a chance-constrained optimization program of the same type as that considered in [19], [20], [21]. Worst-case minimization, as opposed to average minimization, seems to be preferable to obtain the robust satisfaction of spatio-temporal requirements as specified by TWs. Moreover, by choosing ϵ, the robustness level can be tuned by the user according to the desired level of risk for the specific situation at hand. To handle the resulting probabilistic constraints, we resort to the scenario approach, [22], [23], [24], [25], which allows one to find approximate but guaranteed solutions to chance-constraint optimization problems at low computational effort. In particular, we rely on the approaches of [26], [19], [21], [27], [20], where the scenario approach is tailored to the receding horizon framework. This way, convexity is eventually recovered in the optimization problem, which can be efficiently solved at every time step. The so obtained receding horizon control scheme is well performing and robust with respect to wind, as it clearly appears from the numerical simulations.

This work further extends our previous work in [28] where a simpler dynamic is considered and no stochastic wind perturbation is accounted for, while pursuing a regulation – not a trajectory tracking – problem. Further developments are presented in our more recent work in [29] where the wind model was included. The current manuscript extends [28], [29] in several directions. More specifically, introduction and problem position are better motivated, referring to the relevant literature. A thorough discussion on the application of the scenario approach, including numerical implementation issues is given. Many technical aspects involved in the feedback linerization and constraints convexification procedures, which were omitted in the conference publications, are here detailed. A more extensive simulation section showing the performance of the resulting stochastic receding horizon optimization scheme is presented.

The main novel contribution of this work with respect to the related literature is that nonlinear dynamics, confort and actuation constraints, the presence of wind disturbance, and spatio-temporal constraints are jointly accounted for in the design of a strategy to navigate an aircraft through the airspace. This is achieved by integrating feedback linearization and constrained control within a receding horizon implementation, where robustness against the spatially and time varying wind uncertainty is obtained by combining the on-line identification of a local wind model with scenario optimization.

The rest of the paper is organized as follows. In Section II we describe the model of the aircraft, the constraints on the state and control variables as induced by physical limitations and passengers comfort, and the wind disturbance model. In Section III we apply feedback linearization to the aircraft model and reformulate the constraints in the new state and input variables, eventually introducing suitable convex relaxations. In Section IV we address the design of the aircraft control via the receding horizon approach, and adopt an approximate local model for the wind and the scenario approach for coping with uncertainty. Simulation results are reported in Section V. Concluding remarks are drawn in Section VI.

II. Models of the aircraft and wind disturbance

A. Aircraft dynamics

We consider a flat earth, point mass model for the aircraft dynamics, as suggested in [18], [30], [31], [32]. The state variables are given by the position of the aircraft expressed in Cartesian coordinates x, y, z with respect to a fixed frame, the True Air Speed (TAS) of the aircraft V (which is the relative aircraft speed with respect to the surrounding air), the heading angle ψ (which is the angle between the projection of the aircraft velocity on the x-y plane and the x-axis), the path angle γ (which is the angle between the velocity and the x-y plane) and the mass m of the aircraft. The inputs are the Angle of Attack (AoA) α (which is the difference between the pitch and the path angles), the bank angle ϕ (which is the angle between the lift force and the plane containing the aircraft velocity and the z-axis), and the engine thrust T. The presence of the wind is modelled by adding a disturbance $(w_x,\, w_y,\, w_z)$ to the aircraft velocity along the x, y, z axes respectively. The system evolves according to the following equations

$$\begin{bmatrix} \dot{x} \\ \dot{y} \\ \dot{z} \\ \dot{V} \\ \dot{\psi} \\ \dot{\gamma} \\ \dot{m} \end{bmatrix} = \begin{bmatrix} V\cos\psi\cos\gamma + w_x \\ V\sin\psi\cos\gamma + w_y \\ V\sin\gamma + w_z \\ -\frac{D}{m} - g\sin\gamma + \frac{T\cos\alpha}{m} \\ \frac{L+T\sin\alpha}{mV\cos\gamma}\sin\phi \\ \frac{L+T\sin\alpha}{mV}\cos\phi - \frac{g}{V}\cos\gamma \\ -\eta T \end{bmatrix}, \tag{1}$$

where g is gravitational acceleration, η is a fuel consumption coefficient, $D(z,V,\alpha) = \frac{1}{2}\rho(z)SV^2\ C_d(1 + b_1\alpha + b_2\alpha^2)$ is the drag force that opposes the aircraft motion in the direction of the TAS and $L(z,V,\alpha) = \frac{1}{2}\rho(z)SV^2C_l(1 + a\alpha)$ is the lift that provides the force to oppose gravity. In the expression

for D and L, ρ is the air density which is a function of the altitude z, S is the surface of the wings, and C_d, C_l, b_1, b_2, a are suitable positive aerodynamics coefficients.

It is worth noticing that model (1) is well defined and representative of the aircraft dynamics on a specific domain only. More precisely, the states x, y, z can take value in $\mathbb{R}^3$, instead the TAS has to be positive $V \in (0, +\infty)$, the heading angle can take any value in $\mathbb{R}$, but, since it is an angle, we can limit its domain to $\psi \in [0, 2\pi)$, the path angle can take values $\gamma \in (-\pi/2, \pi/2)$, and $m \in (0, +\infty)$. Indeed, being the TAS a speed, it cannot be negative, and if it is null the heading and the path angle become not well defined. Moreover, also when the velocity is aligned with the z-axis ($\gamma = \pm\pi/2$) the heading angle is not well defined. As for the inputs we consider that T must be non negative $T \in [0, +\infty)$, the bank angle and the angle of attack are limited to interval $(-\pi/2, \pi/2)$.

In order to account for physical limitations of the aircraft, comfort and safety requirements, several constraints both on the state variables and on the input variables have to be considered as follows, [32].

- Vertical Acceleration $\ddot{z}$ [1]

$$-a_Z \leq \ddot{z} \leq a_Z. \tag{2}$$

- True Air Speed V

$$V_{min} \leq V \leq V_{max}, \tag{3}$$

  where V_{min} and V_{max} depend on the aircraft type; V_{min} is also related to the stall velocity of the aircraft.
- Longitudinal Acceleration

$$-a_L \leq \dot{V} \leq a_L. \tag{4}$$

- Engine Thrust T

$$T_{min} \leq T \leq T_{max}, \tag{5}$$

  where T_{min} and T_{max} can be computed according to [32] and depend on atmospheric conditions and aircraft type.
- Bank Angle ϕ

$$-\bar{\phi} \leq \phi \leq \bar{\phi}. \tag{6}$$

  According to [32] $\bar{\phi}$ can vary from $25°$ to $45°$ depending on the type of aircraft.
- Path Angle γ

$$\gamma_{min} \leq \gamma \leq \gamma_{max}, \tag{7}$$

  where γ_{min} and γ_{max} must be chosen according to the following reasoning. If the path angle is set to γ_{min} [γ_{max}] and the engine thrust is kept at its minimum T_{min} [at its maximum T_{max}], then the TAS V remains smaller than V_{max} [larger than V_{min}].

[1] In [32] the following constraint is considered

$$-a_N \leq \frac{\Delta\gamma V}{\Delta t} \leq a_N,$$

which limits the normal acceleration. Here, we translate it directly into a bound on the vertical acceleration $\ddot{z}$, taking into account the limitations of γ in (7).

B. Wind model

The wind velocities w_x, w_y, w_z are modelled as a time varying vector field ($w_x = w_x(x, y, z, t)$, $w_y = w_y(x, y, z, t)$, $w_z = w_z(x, y, z, t)$) obtained as the sum of two contributions: a deterministic term that represents the forecast of the wind, and a stochastic term accounting for the mismatch between forecast and the actual wind encountered by the aircraft, that is:

$$w_x = w_{xf} + w_{xs} \quad w_y = w_{yf} + w_{ys} \quad w_z = w_{zf} + w_{zs}.$$

As for the forecast, we rely on the National Oceanic and Atmospheric Administration (NOAA) Rapid Refresh (RAP) model [17] which provides the wind velocities w_{xf}, w_{yf}, w_{zf} in correspondence of a grid of points in the x-y-z space. The forecast has a time resolution of 1 hour. As for the x, y coordinates, the grid has a fixed resolution of 13 km, while as for the z coordinate the grid has a x-y position and time dependent resolution: for each sampled time instant and for each x-y in the grid, the z coordinate is divided in 37 levels each corresponding to a decrease of pressure of 2500 Pa. In order to retrieve the value of the wind velocities $w_{xf} = w_{xf}(x, y, z, t)$, $w_{yf} = w_{yf}(x, y, z, t)$, $w_{zf} = w_{zf}(x, y, z, t)$ in the generic position (x, y, z) at the generic time t, we perform a linear interpolation of the forecast wind velocities in correspondence of the points of the grid at the vertices of the cell containing (x, y, z), and, then, we linearly interpolate over time.

As for the stochastic wind components, in order to account for both the space correlation of the wind (for a fixed time instant, the closer are two points in space, the more similar are the wind velocities at those points) and the time correlation (for a fixed position, the closer the time instants, the more similar the velocities at these time instants), we adopt the same model of [18], [10], where (w_{xs}, w_{ys}, w_{zs}) is assumed to be a time varying random field with a correlation that exponentially decays with distance and with time. Specifically, for every x, y, z, t, the wind components $w_{xs}(x, y, z, t)$, $w_{ys}(x, y, z, t)$, $w_{zs}(x, y, z, t)$ are zero mean Gaussian random variables with the following spatio-temporal correlation structure:

$$\begin{aligned}
&\mathbb{E}[w_{xs}(x,y,z,t)w_{xs}(x',y',z',t')] = \\
&\quad k(z)k(z')e^{-\sigma_1|t-t'|}e^{-\sigma_2\|[x-x'\ y-y']\|}e^{-\sigma_3|z-z'|} \\
&\mathbb{E}[w_{ys}(x,y,z,t)w_{ys}(x',y',z',t')] = \\
&\quad k(z)k(z')e^{-\sigma_1|t-t'|}e^{-\sigma_2\|[x-x'\ y-y']\|}e^{-\sigma_3|z-z'|} \\
&\mathbb{E}[w_{zs}(x,y,z,t)w_{zs}(x',y',z',t')] = \\
&\quad k_z(z)k_z(z')e^{-\sigma_{1z}|t-t'|}e^{-\sigma_{2z}\|[x-x'\ y-y']\|}e^{-\sigma_{3z}|z-z'|} \\
&\mathbb{E}[w_{xs}(x,y,z,t)w_{ys}(x',y',z',t')] = 0 \\
&\mathbb{E}[w_{xs}(x,y,z,t)w_{zs}(x',y',z',t')] = 0 \\
&\mathbb{E}[w_{ys}(x,y,z,t)w_{zs}(x',y',z',t')] = 0
\end{aligned} \tag{8}$$

for all x, y, z, t, x', y', z', t', where $k(z)$ and $k_z(z)$ represent the variance of the wind velocities at a given altitude z and the coefficients σ_1, σ_2, σ_3 and σ_{1z}, σ_{2z}, σ_{3z} regulate the exponential decrease of the correlation between wind velocities at different positions and time instants as their corresponding spatial and temporal distance increases.

According to the correlation structure in (8), wind velocities along different axes are independent and, moreover, wind is isotropic with respect to x, y, i.e. the correlation structure is invariant under rotations of the x-y plane. As a matter of fact, the correlation function in (8) is the same for w_{xs} and w_{ys} while w_{zs} has its own correlation function. Note that according to this model the wind disturbance has unbounded support. Perhaps, it is worth noticing from the outset that we shall use this random vector field characterization of the wind velocity for simulation purposes in validating our strategy in Section V, whereas the strategy itself will be designed based on a local wind model identified on-line (see Section IV-B). A possible approach to generate samples of a random field that satisfy the correlation structure in (8) is described in [18], [10].

III. Feedback linearization and reformulation of the constraints

A. Feedback linearization

In this section, feedback linearization is applied to (1) so as to make the deterministic part of the model of the aircraft linear with respect to some new set of input and state variables. The obtained model is discretized so as to easy to handle in the receding horizon framework. Interestingly, the obtained linear model is very easy to interpret since it describes the evolution of the aircraft position in Cartesian coordinates with the respective accelerations as (new) control inputs.

We start by simplifying (1) by neglecting the mass dynamics, since it is quite slow with respect to the other variables dynamics and it is not a controlled variable in our set-up.

We then define the new state variables as follows:

$$\begin{array}{ll} x_1 = x & x_4 = V\cos\psi\cos\gamma \\ x_2 = y & x_5 = V\sin\psi\cos\gamma \\ x_3 = z & x_6 = V\sin\gamma \end{array} \tag{9}$$

As anticipated above, the new state variables have a precise physical meaning: x_1, x_2, x_3 give the position of the aircraft in Cartesian coordinates, while x_4, x_5, x_6 represent the aircraft velocity Cartesian components. Moreover (9) is clearly a bijection and the original state variables can be recovered from the new ones according to the following inverse relation:

$$\begin{array}{ll} x = x_1 & V = \sqrt{x_4^2 + x_5^2 + x_6^2} \\ y = x_2 & \psi = \arg(x_4, x_5) \\ z = x_3 & \gamma = \arcsin\left(\frac{x_6}{\sqrt{x_4^2+x_5^2+x_6^2}}\right), \end{array} \tag{10}$$

where $\arg(x_4, x_5)$ denotes the phase of the complex number $x_4 + ix_5$ in $[0, 2\pi)$.

Our goal is now to first derive the description of the system in the new state variables, and then define the control inputs, i.e., the AoA α, the bank angle ϕ, and the engine thrust T, as a function of the state and new control input variables so as to obtain a linear model.

To this purpose we start by setting the engine thrust T to:

$$T = (D + mg\sin\gamma + \tau m)\frac{1}{\cos\alpha}, \tag{11}$$

where τ is a new auxiliary input replacing the thrust T. Substituting in (1), the dynamics of V becomes:

$$\dot{V} = \tau. \tag{12}$$

Note that τ represents the part of the acceleration provided by the engine thrust that is still available once the drag force and the projection of the weight force along the path have been compensated.

Differentiating (9) and using (1), (11) and (12), we can derive the following equations governing the new state variables evolution:

$$\begin{aligned} \dot{x}_1 &= x_4 + w_x \\ \dot{x}_2 &= x_5 + w_y \\ \dot{x}_3 &= x_6 + w_z \\ \dot{x}_4 &= \tau\cos\gamma\cos\psi - V\cos\gamma\sin\psi\left(\tfrac{L+T\sin\alpha}{mV\cos\gamma}\sin\phi\right) \\ &\quad - V\sin\gamma\cos\psi\left(\tfrac{L+T\sin\alpha}{mV}\cos\phi - \tfrac{g}{V}\cos\gamma\right) \\ \dot{x}_5 &= \tau\cos\gamma\sin\psi + V\cos\gamma\cos\psi\left(\tfrac{L+T\sin\alpha}{mV\cos\gamma}\sin\phi\right) \\ &\quad - V\sin\gamma\sin\psi\left(\tfrac{L+T\sin\alpha}{mV}\cos\phi - \tfrac{g}{V}\cos\gamma\right) \\ \dot{x}_6 &= \tau\sin\gamma + V\cos\gamma\left(\tfrac{L+T\sin\alpha}{mV}\cos\phi - \tfrac{g}{V}\cos\gamma\right). \end{aligned} \tag{13}$$

If we define as new input variables u_1, u_2, u_3:

$$\begin{aligned} u_1 = {} & \tau\cos\gamma\cos\psi - V\cos\gamma\sin\psi\left(\tfrac{L+T\sin\alpha}{mV\cos\gamma}\sin\phi\right) \\ & -V\sin\gamma\cos\psi\left(\tfrac{L+T\sin\alpha}{mV}\cos\phi - \tfrac{g}{V}\cos\gamma\right) \end{aligned} \tag{14a}$$

$$\begin{aligned} u_2 = {} & \tau\cos\gamma\sin\psi + V\cos\gamma\cos\psi\left(\tfrac{L+T\sin\alpha}{mV\cos\gamma}\sin\phi\right) \\ & -V\sin\gamma\sin\psi\left(\tfrac{L+T\sin\alpha}{mV}\cos\phi - \tfrac{g}{V}\cos\gamma\right) \end{aligned} \tag{14b}$$

$$u_3 = \tau\sin\gamma + V\cos\gamma\left(\tfrac{L+T\sin\alpha}{mV}\cos\phi - \tfrac{g}{V}\cos\gamma\right), \tag{14c}$$

then, the last three equations in (13) become linear, thus leading to:

$$\begin{bmatrix}\dot{x}_1\\ \dot{x}_2\\ \dot{x}_3\\ \dot{x}_4\\ \dot{x}_5\\ \dot{x}_6\end{bmatrix} = \begin{bmatrix}0_{3\times3} & I_3\\ 0_{3\times3} & 0_{3\times3}\end{bmatrix}\begin{bmatrix}x_1\\ x_2\\ x_3\\ x_4\\ x_5\\ x_6\end{bmatrix} + \begin{bmatrix}0_{3\times3}\\ I_3\end{bmatrix}\begin{bmatrix}u_1\\ u_2\\ u_3\end{bmatrix} + \begin{bmatrix}I_3\\ 0_{3\times3}\end{bmatrix}\begin{bmatrix}w_x\\ w_y\\ w_z\end{bmatrix}. \tag{15}$$

Note that, likewise x_1, x_2, x_3, x_4, x_5, x_6, the new inputs u_1, u_2, u_3 have a precise physical meaning being the Cartesian components of the aircraft acceleration with respect to the air.

To ease subsequent developments, system (15) is discretized by applying a constant input in the interval $[t, t+T_s)$, where T_s is the sample time, so obtaining:

$$\mathbf{x}_{k+1} = A\mathbf{x}_k + B\mathbf{u}_k + B_w\mathbf{w}_k \tag{16}$$

where $\mathbf{x}_k = [x_{1,k}, x_{2,k}, x_{3,k}, x_{4,k}, x_{5,k}, x_{6,k}]^T$ is the state vector, $\mathbf{u}_k = [u_{1,k}, u_{2,k}, u_{3,k}]^T$ is the input vector and $\mathbf{w}_k = [w_{1,k}, w_{2,k}, w_{3,k}]^T$ is the disturbance vector and we set

$$A = \begin{bmatrix}I_3 & T_sI_3\\ 0_{3\times3} & I_3\end{bmatrix} \quad B = \begin{bmatrix}\frac{T_s^2}{2}I_3\\ T_sI_3\end{bmatrix} \quad B_w = \begin{bmatrix}T_sI_3\\ 0_{3\times3}\end{bmatrix}.$$

Derivation of the state feedback linearizing control law

In order to retain the validity of the linear model (15), it remains to show that, for any admissible value of u_1, u_2, and u_3, admissible values for the original inputs of the aircraft model τ, ϕ and α can be found so that (14a)-(14c) are met. We next show that equations (14a)-(14c) can indeed be solved for τ, ϕ and α as function of the new inputs u_1, u_2, u_3 and of the state variables x, y, z, V, ψ, γ, thus obtaining the nonlinear feedback control law linearizing (13).

Calculating $u_1 \cos\psi + u_2 \sin\psi$ and $-u_1 \sin\psi + u_2 \cos\psi$ from (14a) and (14b) gives:

$$\tau = \frac{1}{\cos\gamma}\big(u_1 \cos\psi + u_2 \sin\psi + \sin\gamma\big(\frac{L + T\sin\alpha}{m}\cos\phi - g\cos\gamma\big)\big) \quad (17)$$

$$(L + T\sin\alpha)\sin\phi = m\left(-u_1 \sin\psi + u_2 \cos\psi\right), \quad (18)$$

while from (14c) we have that:

$$\frac{L + T\sin\alpha}{mV}\cos\phi - \frac{g}{V}\cos\gamma = \frac{u_3 - \tau\sin\gamma}{V\cos\gamma}, \quad (19)$$

which is the same as:

$$(L + T\sin\alpha)\cos\phi = m\frac{u_3 - \tau\sin\gamma + g\cos^2\gamma}{\cos\gamma}. \quad (20)$$

Using (19) in (17) and solving for τ yields:

$$\tau = \cos\gamma(u_1\cos\psi + u_2\sin\psi + u_3\tan\gamma). \quad (21)$$

To ease the notation define the auxiliary variables:

$$\nu_1 = u_3 - \tau\sin\gamma + g\cos^2\gamma \quad (22)$$
$$\nu_2 = -u_1\sin\psi + u_2\cos\psi,$$

so that (18) and (20) rewrites as:

$$(L + T\sin\alpha)\sin\phi = m\nu_2 \quad (23)$$

$$(L + T\sin\alpha)\cos\phi = \frac{m}{\cos\gamma}\nu_1 \quad (24)$$

If $\nu_1 \neq 0$, then the bank angle ϕ can be computed as:

$$\phi = \arctan\left(\frac{\nu_2\cos\gamma}{\nu_1}\right) \in \left(-\frac{\pi}{2}, \frac{\pi}{2}\right), \quad (25)$$

which is exactly the domain of ϕ. If $\nu_1 = 0$, then ν_2 must be 0 as well, because, otherwise, $\nu_1 = 0$ and $\nu_2 \neq 0$ would imply $\phi = \pm\pi/2$ while we imposed that $\phi \in (-\pi/2, \pi/2)$. In the case when $\nu_1 = 0$ and $\nu_2 = 0$, it turns out that $L + T\sin\alpha = 0$ so that ϕ can be arbitrarily chosen. Note that if $L + T\sin\alpha = 0$, then the value of ϕ does not affect the system dynamics, see (1). To fix a value we set $\phi = 0$ when $\nu_1 = 0$ and $\nu_2 = 0$.

Since $\phi \in (-\pi/2, \pi/2)$, $L + T\sin\alpha$ must take the same sign of ν_1, hence, substituting the expressions for $\sin\phi$ and for $\cos\phi$ given by (23), (24) into the equation $\sin^2\phi + \cos^2\phi = 1$ one recovers:

$$L + T\sin\alpha = m\sqrt{\frac{\nu_1^2}{\cos^2\gamma} + \nu_2^2}\cdot \operatorname{sign}(\nu_1). \quad (26)$$

Substituting in (26) the expression of T given in (11) and writing explicitly the dependence of L and D on α, it is then seen that the AoA α has to satisfy the following equation:

$$m\sqrt{\frac{\nu_1^2}{\cos^2\gamma} + \nu_2^2}\operatorname{sign}(\nu_1) = \tfrac{1}{2}\rho S V^2 C_l(1 + a\alpha) + \big(m\tau + gm\sin\gamma + \tfrac{1}{2}\rho S V^2 C_d(1 + b_1\alpha + b_2\alpha^2)\big)\tan\alpha. \quad (27)$$

If equation (27) admits a solution, then, there exists a value of α such that the aircraft dynamics is feedback linearized. This is the case if the right-hand side of (27) spans all the values between $-\infty$ and $+\infty$ as α varies in the range $(-\pi/2, \pi/2)$. Note that the right-hand side of (27) is a continuous function of α, given by the sum of a linear term in α and a quadratic term in α multiplied by $\tan\alpha$. Hence, since the image of the linear term is bounded for $\alpha \in (-\pi/2, \pi/2)$, the sought property is obtained if and only if the quadratic term multiplied by $\tan\alpha$ tends to $-\infty$ and $+\infty$ as α approaches $-\pi/2$ and $\pi/2$. To obtain this, since the coefficient multiplying α^2 is positive (recall that all aerodynamic coefficients C_l, a, C_d, b_1, b_2 are positive), a sufficient condition is that the roots α_1 and α_2 of the quadratic term are either not real or, if real, both strictly inside $(-\pi/2, \pi/2)$. Indeed, if α_1 and α_2 are not real, then the quadratic term is always positive, while if instead α_1 and α_2 are real with $-\pi/2 < \alpha_1 < \alpha_2 < \pi/2$, then, the quadratic term takes positive values in the intervals $(-\pi/2, \alpha_1)$ and $(\alpha_2, \pi/2)$. In both cases the quadratic term multiplied by $\tan\alpha$ tends to $-\infty$ and $+\infty$ as α approaches $-\pi/2$ and $\pi/2$.[2] Requiring that the roots of the quadratic term are real and belong to $(-\pi/2, \pi/2)$ amounts to have

$$\begin{cases} (C_d b_1)^2 - 4C_d b_2\left(C_d + m\frac{\tau + g\sin\gamma}{\frac{1}{2}\rho S V^2}\right) \geq 0 \\ \dfrac{-C_d b_1 - \sqrt{(C_d b_1)^2 - 4C_d b_2\left(C_d + m\frac{\tau + g\sin\gamma}{\frac{1}{2}\rho S V^2}\right)}}{2C_d b_2} > -\frac{\pi}{2}, \end{cases}$$

where, if $\pi b_2 - b_1 > 0$, the second inequality can be rewritten as:

$$m(\tau + g\sin\gamma) > \left(-\frac{\pi^2}{4}b_2 + \frac{\pi}{2}b_1 - 1\right)\frac{1}{2}\rho S V^2 C_d. \quad (28)$$

In principle, this may limit the domain of validity of the feedback linearization. However, this is not the case for standard aircraft operating conditions since (28) is automatically satisfied when the constraints of Section II-A are enforced (see the example in Section V).

In principle, when solving (27), we may find a value for α that maps into a negative engine thrust T when plugged into (11). However, this is not an admissible solution since it is not compatible with constraint (5) on T. Interestingly, if equation (27) has a solution that corresponds to $T > 0$, then, this solution is unique. In order to prove this property, we shall show that the right-hand side of (27) is monotonically

[2]It is worth noticing that this argument is for the purpose of proving existence of a solution α and it does not imply that α takes a value close to either $-\pi/2$ or $+\pi/2$. On the contrary, in normal aircraft operations, the right-hand-side of (26) is almost completely compensated by the lift L and, correspondingly, the AoA α takes small values.

increasing with α when $T > 0$. To this purpose, we compute the derivative of the right-hand side of (27) with respect to α:

$$\frac{\frac{1}{2}\rho S V^2 C_l a + \left(m\tau + gm\sin\gamma + \frac{1}{2}\rho S V^2 C_d(1 + b_1\alpha + b_2\alpha^2)\right)}{\frac{1}{\cos^2\alpha}} + \left(\frac{1}{2}\rho S V^2 C_d(b_1 + 2b_2\alpha)\right)\tan\alpha, \quad (29)$$

and analyze when it is positive. The term $m\tau + gm\sin\gamma + \frac{1}{2}\rho S V^2 C_d(1+b_1\alpha+b_2\alpha^2) = T\cos\alpha$ is positive when $T > 0$, so that a sufficient condition for (29) to be positive is:

$$aC_l + C_d(b_1 + 2b_2\alpha)\tan\alpha > 0. \quad (30)$$

Note that since the coefficients C_d, b_1, b_2 are positive, the term $C_d(b_1 + 2b_2\alpha)\tan\alpha$ is not positive only for $\alpha \in [-\frac{b_1}{2b_2}, 0]$, and in this interval $C_d(b_1 + b_2\alpha)\tan\alpha \geq -C_d b_1 \tan\left(\frac{b_1}{2b_2}\right)$. In view of this, a sufficient condition to ensure that (30) holds is:

$$aC_l - C_d \tan\left(\frac{b_1}{2b_2}\right) b_1 > 0.$$

This condition is usually satisfied because a and C_l are positive and, moreover, $C_l \gg C_d$ for standard aircraft.

In conclusion, equation (27) admits a solution in α, and this solution is unique in the considered range of aircraft operation, as specified by the constraint is Section II-A.

To find α as a function of the other variables, equation (27) can be solved numerically, e.g. by bisection. This along with equations (11), (21), (22) and (25), gives the (nonlinear) feedback that makes the dynamics of x_1, x_2, x_3, x_4, x_5, x_6 linear with respect to the new inputs u_1, u_2, u_3 (see (15)).

B. Reformulation of the constraints in the new variables

Recall that our goal is implementing a control strategy for trajectory tracking, by formulating a suitable finite horizon constrained optimization problem that is repeatedly solved on-line over a receding horizon. It is then fundamental for computational and solvability reasons to achieve convexity. To this purpose, in the previous section we applied feedback linearization to rewrite the aircraft model as a linear system. This has undoubtedly the advantage of simplifying the design. On the other hand, constraints (2)-(7), which must be enforced for a proper operation of the aircraft, remain non-convex even when rewritten in terms of new state and input variables x_1, x_2, x_3, x_4, x_5, x_6, u_1, u_2, u_3.

The aim of this section is then to first reformulate the constraints over a finite horizon in view of subsequent receding horizon control implementation, and then to introduce suitable relaxations, when needed, in order to convexify them. Relaxation is conceived in such a way that any original constraint is guaranteed to be satisfied at the first instant of the considered time horizon (k for $\mathbf{u}$ and $k+1$ for $\mathbf{x}$). In this way, since in the receding horizon implementation only the input designed for the first time instant is applied and then optimization is repeated over the new, 1-time step ahead, time horizon, the original constraints are met at every time instant by the actual control action that is implemented.

We next consider one by one the constraints introduced in Section II-A. The convexified constraints will all be linear except one.

Vertical Acceleration

Since the input u_3 is equal to the vertical acceleration $\ddot{z}$, constraint (2) can be straightforwardly written as:

$$-a_Z \leq u_{3,k+i} \leq a_Z \qquad i = 0, \ldots, M-1. \quad (31)$$

True Air Speed V

Being $V^2 = x_4^2 + x_5^2 + x_6^2$, constraints (3) on TAS is rewritten as:

$$x_{4,k+i}^2 + x_{5,k+i}^2 + x_{6,k+i}^2 \leq V_{max}^2 \qquad i = 1, \ldots, M \quad (32)$$
$$x_{4,k+i}^2 + x_{5,k+i}^2 + x_{6,k+i}^2 \geq V_{min}^2 \qquad i = 1, \ldots, M. \quad (33)$$

Constraints (32) are already convex, and their interpretation is that the aircraft velocity[3] lies inside a sphere of radius V_{max}. Constraints (33) are instead concave as they require that the aircraft velocity lies outside a sphere of radius V_{min}. To attain convexity, constraints (33) are modified by requiring that the aircraft velocity stays beyond a plane tangent to sphere of radius V_{min} and oriented according to the current, i.e. at time k, heading angle ψ_k and path angle γ_k, which are available since the state is measurable. The new constraints can be expressed by means of the following linear inequalities:

$$\begin{bmatrix}1 & 0 & 0\end{bmatrix} R_y R_z \begin{bmatrix}x_{4,k+i}\\ x_{5,k+i}\\ x_{6,k+i}\end{bmatrix} \geq V_{min} \quad i = 1, \ldots, M, \quad (34)$$

where the rotation matrices $R_z(\psi_k)$ and $R_y(\gamma_k)$ are defined as:

$$R_z = \begin{bmatrix}\cos\psi_k & \sin\psi_k & 0\\ -\sin\psi_k & \cos\psi_k & 0\\ 0 & 0 & 1\end{bmatrix}$$

$$R_y = \begin{bmatrix}\cos\gamma_k & 0 & \sin\gamma_k\\ 0 & 1 & 0\\ -\sin\gamma_k & 0 & \cos\gamma_k\end{bmatrix}.$$

Note that (32) and (34) together pose a stricter condition than (32) and (33), so that the original constraints are always satisfied. The drawback with (34) is that, having the plane tangent to the sphere of radius V_{min} fixed orientation, for values of TAS close to V_{min}, the aircraft is forced to accelerate in order to turn in the finite horizon problem. However this side-effect is negligible for higher values of TAS, which correspond to the usual flight conditions, and, moreover, thanks to the receding horizon strategy, the plane orientation is recomputed at each time step according the current values of ψ_k and γ_k, and this drawback is further mitigated in the actual trajectory of the aircraft.

Longitudinal Acceleration

From $\dot{V} = \tau$ and (21), constraint (4) on longitudinal acceleration rewrites as:

$$-a_L \leq \cos\gamma_{k+i}(\cos\psi_{k+i}u_{1,k+i} + \sin\psi_{k+i}u_{2,k+i} + \tan\gamma_{k+i}u_{3,k+i}) \leq a_L,\ i = 0, \ldots, M-1.$$

[3]Note that the aircraft velocity with respect to the surrounding air is a vector with modulus equal to V and orientation given by the heading angle ψ and by the path angle γ. Its Cartesian components are x_4, x_5, x_6.

Further substituting the expressions for γ_{k+i} and ψ_{k+i} as functions of $x_{4,k+i}$, $x_{5,k+i}$, $x_{6,k+i}$ as in (10), it is easily seen that the constraints are not convex. We decide then to approximate them by replacing the values of the heading angle ψ_{k+i} and of the path angle γ_{k+i} with their initial values ψ_k and γ_k, which are available. This approximation seems to be acceptable for the heading angle cannot vary too much in the considered finite time horizon while, given the limitations on it, the path angle always keeps close to 0. This yields:

$$\begin{aligned} -a_L \leq &\cos\gamma_k(u_{1,k+i}\cos\psi_k + u_{2,k+i}\sin\psi_k \\ &+ u_{3,k+i}\tan\gamma_k) \leq a_L,\ i=0,\dots,M-1, \end{aligned} \tag{35}$$

which are linear constraints on the input vector $\mathbf{u}_{k+i}$, $i = 0,\dots,M-1$. Notably, for $i=0$, the constraint on $\mathbf{u}_k$ is exactly equivalent to the original one, without any approximation. Thus, if the control input is designed to satisfy (35), and a receding horizon is considered, then the original constraint (4) is not violated by the actual aircraft motion because each time only the first $\mathbf{u}_k$ is indeed applied.

Path Angle γ

Recalling that $x_6 = V\sin(\gamma)$ the constraint (7) writes as

$$V_{k+i}\sin\gamma_{min} \leq x_{6,k+i} \leq V_{k+i}\sin\gamma_{max},\ i=1,\dots,M, \tag{36}$$

which is however non-convex because

$$V_{k+i} = \sqrt{x_{4,k+i}^2 + x_{5,k+i}^2 + x_{6,k+i}^2}.$$

Constraint (36) can be approximated by keeping V fixed to its initial value V_k for all $i=1,\dots,M$, leading to

$$V_k\sin\gamma_{min} \leq x_{6,k+i} \leq V_k\sin\gamma_{max} \quad i=1,\dots,M. \tag{37}$$

Although the approximation is mild as V cannot vary too much along the prediction horizon, note, however that (37) does not guarantee the satisfaction of the original constraint (7), not even for $i=1$. Hence, we prefer to tackle (36) by replacing V_{k+i} with the worst-case prediction of its values along the considered prediction horizon. Given the constraints (3) and (4) on TAS and on the longitudinal acceleration, the maximal decrease of TAS over the prediction horizon is

$$V_{k+i}^{wc^-} = \max\{V_k - iT_s a_L, V_{min}\} \quad i=0,\dots,M,$$

while the maximal increase is

$$V_{k+i}^{wc^+} = \min\{V_k + iT_s a_L, V_{max}\} \quad i=0,\dots,M.$$

Turning back to (36), since $\sin\gamma_{min}$ is negative and $\sin\gamma_{max}$ is positive the worst-case is achieved when V_{k+i} takes the smallest values, which leads to enforce the constraints

$$V_{k+i}^{wc^-}\sin\gamma_{min} \leq x_{6,k+i} \leq V_{k+i}^{wc^-}\sin\gamma_{max} \quad i=1,\dots,M, \tag{38}$$

in place of (36). The constraints in (38) pose a stricter condition than (36), so that when (38) is applied the satisfaction of the original constraint is guaranteed along the whole prediction horizon. A compromise between (37) and (38) consist in fixing V to the first step worst case prediction $V_{k+1}^{wc^-}$, that is:

$$V_{k+1}^{wc^-}\sin\gamma_{min} \leq x_{6,k+i} \leq V_{k+1}^{wc^-}\sin\gamma_{max} \quad i=1,\dots,M. \tag{39}$$

This way the original constraint is guaranteed for $i=1$ only, but its satisfaction along all the aircraft operation is recovered thanks to receding horizon. On the other hand, the conservatism introduced by worst case safeguarding is mitigated and a better performance is achieved.

Bank Angle ϕ

In view of (18), the constraint (6) on the bank angle can be rewritten as:

$$\begin{aligned} &|-\sin\psi_{k+i}u_{1,k+i} + \cos\psi_{k+i}u_{2,k+i}| \\ &\leq \sin\bar{\phi}\frac{L_{k+i} + T_{k+i}\sin\alpha_{k+i}}{m},\ i=0,\dots,M-1. \end{aligned} \tag{40}$$

Taking the squares and recalling (26), (22), we get:

$$\nu_{2,k+i}^2 \leq \sin^2\bar{\phi}\left(\frac{\nu_{1.t+i}^2}{\cos^2\gamma_{k+i}} + \nu_{2,k+i}^2\right),\ i=0,\dots,M-1,$$

which in turn rewrites as

$$\nu_{2,k+i}^2\frac{\cos^2\bar{\phi}}{\sin^2\bar{\phi}}\cos^2\gamma_{k+i} \leq \nu_{1,k+i}^2,\ i=0,\dots,M-1.$$

Recalling the definition of $\nu_{1,k+i}$ and because of the limitations on vertical and longitudinal accelerations, and on the path angle, it can be easily seen than ν_1 and $\cos\gamma$ are always positive.[4] Hence, taking the square root we have

$$|\nu_{2,k+i}|\frac{\cos\bar{\phi}}{\sin\bar{\phi}}\cos\gamma_{k+i} \leq \nu_{1,k+i} \qquad i=0,\dots,M-1,$$

so that replacing the expression of $\nu_{1,k+i}$, $\nu_{2,k+i}$ in (22), the constraints (40) are eventually rewritten as:

$$\begin{aligned} &|-u_{1,k+i}\sin\psi_{k+i} + u_{2,k+i}\cos\psi_{k+i}|\frac{\cos\bar{\phi}}{\sin\bar{\phi}}\cos\gamma_{k+i} \\ &\leq u_{3,k+i} + g\cos^2\gamma_{k+i} - \sin\gamma_{k+i}\cos\gamma_{k+i}(u_{1,k+i}\cos\psi_{k+i} \\ &+ u_{2,k+i}\sin\psi_{k+i} + u_{3,k+i}\tan\gamma_{k+i}),\ i=0,\dots,M-1. \end{aligned}$$

Similarly to previous cases, convexity is recovered replacing ψ_{k+i} and γ_{k+i} with their initial value γ_k and ψ_k:

$$\begin{aligned} &|-\sin\psi_k u_{1,k+i} + \cos\psi_k u_{2,k+i}|\frac{\cos\bar{\phi}}{\sin\bar{\phi}}\cos\gamma_k \\ &\leq u_{3,k+i} + g\cos^2\gamma_k - \sin\gamma_k\cos\gamma_k(\cos\psi_k u_{1,k+i} \\ &+ \sin\psi_k u_{2,k+i} + \tan\gamma_k u_{3,k+i}),\ i=0,\dots,M-1. \end{aligned} \tag{41}$$

Note that, for each i the constraint in (41) is linear and for $i=0$ is exactly equivalent to the original constraint on the bank angle, so that, thanks to receding horizon, the actual aircraft operation can be enforced to satisfies (6) for all time instants through (41).

[4] In particular, note that if $\nu_1 \leq 0$, then $u_3 \leq \tau\sin\gamma - g\cos^2\gamma$, see (22). In this case, given the limitations on the thrust, the vertical acceleration u_3 would be mainly determined by the gravitational force and this would be incompatible with the required flight conditions.

Engine Thrust T

Recalling (11), the constraint on the engine thrust can be written as:

$$T_{min} \leq (m\tau_{k+i} + D(x_{3,k+i}, V_{k+i}, \alpha_{k+i}) + mg\sin\gamma_{k+i})$$
$$\frac{1}{\cos\alpha_{k+i}} \leq T_{max},\ i = 0 \dots M-1,$$

which in turn, by rewriting τ as in (21) and $\sin\gamma = \frac{x_6}{V}$, becomes:

$$T_{min} \leq \Big(m\cos\gamma_{k+i}(u_{1,k+i}\cos\psi_{k+i} + u_{2,k+i}\sin\psi_{k+i} + u_{3,k+i}\tan\gamma_{k+i}) + D(x_{3,k+i}, V_{k+i}, \alpha_{k+i}) + mg\frac{x_{6,k+i}}{V_{k+i}}\Big)\frac{1}{\cos\alpha_{k+i}} \leq T_{max},\ i = 0 \dots M-1. \quad (42)$$

Constraint (42) is non-convex because of its dependence on V_{k+i}, ψ_{k+i}, γ_{k+i}, $x_{3,k+i}$ and α_{k+i}.
We, hence, proceed as follows. As in (35) the value of the heading angle ψ_{k+i} and of the path angle γ_{k+i} are replaced by their initial value ψ_k and γ_k which introduces a mild approximation as discussed above[5]. Likewise, we replace $x_{3,k+i}$ and V_{k+i} with their initial values $x_{3,k}$ and V_k. Again this approximation is sensible because the limitation on the vertical acceleration, on TAS and on the path angle implies that V and x_3 cannot vary too much in the considered finite horizon (note that D depends on x_3 through the function $\rho(x_3)$ which describes how air density varies with altitude and this further reduces the impact of variation of x_3).

Hence the constraint on engine thrust rewrites:

$$T_{min} \leq \Big(m\cos\gamma_k(u_{1,k+i}\cos\psi_k + u_{2,k+i}\sin\psi_k + u_{3,k+i}\tan\gamma_k) + D(x_{3,k}, V_k, \alpha_{k+i}) + mg\frac{x_{6,k+i}}{V_k}\Big)\frac{1}{\cos\alpha_{k+i}} \leq T_{max},\ i = 0 \dots M-1. \quad (43)$$

which is still non-convex because of its dependence on the angle of attack α_{k+i} which is a control input and cannot be set equal to α_k. We then enforce the constraint robustly with respect to all the possible values that α can take as $u_{1,k}$, $u_{2,k}$, $u_{3,k}$ vary while satisfying the other constraints. More precisely, we first compute the admissible range of values for α, $[\underline{\alpha}(\mathbf{x}_k),\ \overline{\alpha}(\mathbf{x}_k)]$, where $\underline{\alpha}(\mathbf{x}_k)$ and $\overline{\alpha}(\mathbf{x}_k)$ are the minimum and the maximum value for α achieved by solving equation (27) when the state is kept fixed to the current value $\mathbf{x}_k$ and the inputs $u_{1,k}$, $u_{2,k}$, $u_{3,k}$ take all the feasible values in accordance to the constraints on the vertical acceleration (31), the longitudinal acceleration (35), the path angle (38), and the bank angle (41). We can then enforce on the engine thrust the robust constraint with respect to the values that can be possibly taken by α:

$$\tilde{T}_{min} \leq mg\frac{x_{6,k+i}}{V_k} + m\cos\gamma_k(u_{1,k+i}\cos\psi_k + u_{2,k+i}\sin\psi_k + u_{3,k+i}\tan\gamma_k) \leq \tilde{T}_{max},\ i = 0, \dots, M-1, \quad (44)$$

[5]Note to this purpose that, though γ_{k+i} keeps close to 0, replacing $\sin\gamma_{k+i}$ with $\sin\gamma_k$ may lead to poor approximation because it is multiplied by a big factor like mg. Hence, it was important to first write $\sin\gamma = \frac{x_6}{V}$ (so that the constraint is actually imposed on x_6) before substituting γ_{k+i} with γ_k.

where we set

$$\tilde{T}_{min} = \max_{\alpha\in[\underline{\alpha}(\mathbf{x}_k),\ \overline{\alpha}(\mathbf{x}_k)]} \{T_{min}\cos\alpha - D(x_{3,k}, V_k, \alpha)\}$$
$$\tilde{T}_{max} = \min_{\alpha\in[\underline{\alpha}(\mathbf{x}_k),\ \overline{\alpha}(\mathbf{x}_k)]} \{T_{max}\cos\alpha - D(x_{3,k}, V_k, \alpha)\}.$$

Remarkably, constraints (44) are linear constraints. Moreover the introduced approximations are such that the original constraints (42) is satisfied for $i = 0$. As a matter of fact, the replacement of ψ_{k+i}, γ_{k+i}, V_{k+i}, $x_{3,k+i}$ with ψ_k, γ_k, V_k, $x_{3,k}$, introduces no error for $i = 0$, while being robust with respect to the values taken by α in correspondence of $\mathbf{x}_k$ implies that (44) for $i = 0$ is a stricter condition than (42) for $i = 0$. This is of most importance because it implies that a control action designed so as to satisfies (44) and implemented along a receding horizon actually satisfies (42) at all time instants.
Note eventually that while computing (44), the admissible range $[\underline{\alpha}(\mathbf{x}_k),\ \overline{\alpha}(\mathbf{x}_k)]$ is adapted to the current state $\mathbf{x}_k$. This introduces a possible error at the subsequent time instants for $i \geq 1$. One possibility would be that of being robust with respect to a larger range of admissible values for α, which is valid for all possible feasible states and not only for the current one. This way constraints guaranteed at all time instants $k+i$, $i = 0, \dots, M-1$ are obtained, but at the same time an extreme conservatism is introduced, which leads to poor performance or even to unfeasibility. The constraint in (44), instead, seems to achieve the best trade off between level of approximation and conservatism and allows one to obtain a good performance.

Concluding remarks

Note that all the derived convex constraints (31), (32), (34), (35), (39), (41), (44) do not depend on the wind disturbance which affects only x_1, x_2, x_3 (see (16)).
Moreover it is perhaps worth noticing that the limitations on path angle posed by $\gamma_{min} = -3^\circ$ and $\gamma_{max} = 5^\circ$ keep the projection of the weight force on the longitudinal direction limited. As it can be easily verified, this ensures that for every admissible operating condition the engine thrust is always (that is without violating the limitations on it) able to counteract the drag and possibly the longitudinal component of the weight force without enforcing the aircraft to increase or decrease the TAS. This means that keeping TAS, heading angle and path angle constant is always feasible. The constraints of this section are then always satisfied by the solution $\mathbf{u}_{k+i} = 0$, $i = 0, \dots, M-1$. This guarantees that the feasibility of the finite horizon optimization problem to be solved at each time instant k is not compromised by the constraints on aircraft physical limitations, safety and passenger comfort discussed in this section.

IV. Receding horizon control strategy

Let (x_1^R, x_2^R, x_3^R), and $(\dot{x}_1^R, \dot{x}_2^R, \dot{x}_3^R)$ denote the reference trajectory and velocity that the aircraft should track. We recall that it is assumed that a perfect tracking of the reference trajectory and velocity guarantees the satisfaction of spatio/temporal constraints as given by TWs. Moreover, the reference trajectory and velocity have been suitably designed

so as to be compatible with the aircraft motion capabilities (see [11] for a possible approach). Given that the aircraft dynamics is affected by wind, the aircraft may deviate from the reference trajectory, which motivates the introduction of a receding horizon controller that steers it back and makes it follow the reference trajectory robustly with respect to the wind disturbance.

A. Finite horizon optimization problem

The main ingredient of our control strategy is the formulation of a suitable finite horizon optimization problem where a suitable cost function J is chosen and possibly additional constraints on the aircraft position are included besides the actuation and comfort constraints discussed in the previous sections.

Given the current time k, we define at each time $k+i$, $i=0,\dots,M$, the position error ξ_{k+i} as the difference between aircraft position $x_{1,k+i}$, $x_{2,k+i}$, $x_{3,k+i}$ and reference position $x^R_{1,k+i}$, $x^R_{2,k+i}$, $x^R_{3,k+i}$. By using the rotation matrix

$$R_z(\psi^R_{k+i}) = \begin{bmatrix} \cos(\psi^R_{k+i}) & \sin(\psi^R_{k+i}) & 0 \\ -\sin(\psi^R_{k+i}) & \cos(\psi^R_{k+i}) & 0 \\ 0 & 0 & 1 \end{bmatrix}$$

associated with the reference heading angle $\psi^R_{k+i} = \arctan(\frac{\dot{x}^R_{1,k+i}}{\dot{x}^R_{2,k+i}})$, we can express the position error ξ_{k+i} in terms of longitudinal, lateral, and vertical components with respect to the reference trajectory:

$$\xi_{k+i} = R_z(\psi^R_{k+i}) \left(\begin{bmatrix} x_{1,k+i} \\ x_{2,k+i} \\ x_{3,k+i} \end{bmatrix} - \begin{bmatrix} x^R_{1,k+i} \\ x^R_{2,k+i} \\ x^R_{3,k+i} \end{bmatrix} \right).$$

One primary objective of the finite horizon optimization problem is to keep the position error ξ_{k+i} as small as possible. Note, however, that ξ_{k+i} depends on the states $x_{1,k+i}$, $x_{2,k+i}$, and $x_{3,k+i}$ which are meant to be replaced by their expressions as functions of the input $\mathbf{u}$ and the disturbance $\mathbf{w}$ computed according to dynamics (16), so that ξ_{k+i} is eventually a function of the wind disturbance: $\xi_{k+i} = \xi_{k+i}(\mathbf{u}_k,\dots,\mathbf{u}_{k+i-1},\mathbf{w}_k,\dots,\mathbf{w}_{k+i-1})$. We should then account for the presence of the wind disturbance in the minimization problem formulation. In this work, we opt for the minimization of the worst-case trajectory tracking errors over all possible wind disturbance realizations except for a set of user-chosen probability ϵ. where $\epsilon \in (0,1)$. Reason is that worst-case minimization, as opposed to average minimization, seems to be preferable for the robust satisfaction of spatio-temporal requirements as specified by TWs. The optimization problem can be posed by introducing $3 \cdot M$ additional optimization variables $h_{L,i}$, $h_{l,i}$, $h_{v,i}$, $i=1,\dots,M$ to be minimized (see the specification of the cost function below) and to enforce that these variables bound the absolute value of the three components of the position error along the prediction horizon with probability $1-\epsilon$, namely:

$$\mathbb{P}\{|\xi_{k+i}| \leq \begin{bmatrix} h_{L,i} \\ h_{l,i} \\ h_{v,i} \end{bmatrix},\ i=1,\dots,M\} \geq 1-\varepsilon, \qquad (45)$$

where the inequality $\leq$ has to be intended component-wise. The violation probability ϵ is a design parameter, which can be modulated to compromise between robustness and tracking performance: in the limit, when ϵ is close to 0, we minimize the tracking accuracy all over all wind disturbance realizations, thus getting a conservative (large) value of the tracking error since the wind disturbance $\mathbf{w}$ has unbounded support. Viceversa, the best tracking accuracy is achieved when ϵ tends to 1, but it is violated by almost all wind disturbance realizations. By selecting a proper ϵ, the user can eventually achieve a proper guaranteed tracking error, which e.g. accomplish with the presence of TWs, and a high enough robustness level for this guarantee.

As for the cost function J, we opt for the sum of two terms: one that depends on the input acceleration $\mathbf{u}$ only and accounts for fuel consumption and passenger comfort, and a second term that accounts for the minimization of the position error thresholds $h_{L,i}$, $h_{l,i}$, $h_{v,i}$, $i=1,\dots,M$ as discussed above. Namely,

$$\begin{aligned} J = \sum_{i=0}^{M-1} \mu^i_{ud} \mathbf{u}^T_{k+i} R \mathbf{u}_{k+i} + \mu_{Lc} \sum_{i=1}^{M} \mu^{i-1}_{Ld} h_{L,i} \qquad (46) \\ + \mu_{lc} \sum_{i=1}^{M} \mu^{i-1}_{ld} h_{l,i} + \mu_{vc} \sum_{i=1}^{M} \mu^{i-1}_{vd} h_{v,i}, \end{aligned}$$

where R, μ_{Lc}, μ_{lc}, μ_{vc}, μ_{ud}, μ_{Ld}, μ_{ld}, μ_{vd} are weights that are now discussed. The weighting matrix R is chosen as follows

$$R = R^T_{rot} R^T_{nor} R_c R_{nor} R_{rot},$$

where

$$R_{rot} = \begin{bmatrix} \cos\psi_k & \sin\psi_k & 0 \\ -\sin\psi_k & \cos\psi_k & 0 \\ 0 & 0 & 1 \end{bmatrix}$$

is a rotation matrix that transforms u_1 and u_2 (namely, the accelerations along the x and y axes) into the longitudinal and lateral accelerations with respect to the initial value of the heading angle ψ_k, whereas $R_{nor} = \text{diag}\left(\frac{1}{a_L}, \frac{1}{g\tan\bar{\phi}}, \frac{1}{a_Z}\right)$ is a normalization matrix, chosen according to the limits on accelerations. Eventually, matrix R_c allows one to weight the longitudinal and lateral accelerations, as well as the vertical acceleration, which are directly related to fuel consumption and comfort. The weight matrix R_c, together with weights μ_{Lc}, μ_{lc}, μ_{vc} regulate the relative importance given to input and position error components, so as to achieve a proper trade-off between saving the control input and keeping the position error small, while the weights μ_{ud}, μ_{Ld}, μ_{ld}, $\mu_{vd} \in (0\ 1]^4$ can be used to give greater importance to the first time steps, which are the most important for the actual aircraft response because of the adopted receding horizon strategy.

Thus, given the discrete-time model of Section III, the convex constraints discussed in Section III-B, the probabilistic constraint in (45) and the cost function (46) described above, the

overall finite horizon optimization problem is as follows:

$$\min_{\substack{\mathbf{u}_{k+i}\ i=0\dots M-1 \\ h_{L,i},\ h_{l,i},\ h_{v,i}\ i=1\dots M}} J \quad \text{subject to:} \tag{47}$$

constraints (31) (32) (34) (35) (39) (41) (44)

$$\mathbb{P}\{|\xi_{k+i}(\mathbf{w}_k,\dots,\mathbf{w}_{k+i-1})| \leq \begin{bmatrix} h_{L,i} \\ h_{l,i} \\ h_{v,i} \end{bmatrix}, i=1,\dots,M\} \geq 1-\varepsilon.$$

Receding horizon control is then obtained by applying the first element $\mathbf{u}_k$ of the computed control actions and repeating the optimization (47) at each time step.

Note that problem (47) is hard to solve because of the presence of the probabilistic constraint and of the complex probabilistic model of the wind, which altogether make it non convex. As a matter of fact, $\mathbf{w}$ is not a standard additive disturbance, but it depends on the aircraft position which in turn is a function of the input to be optimized, as described in Section II-B. In Section IV-B we hence revisit the wind model so that in (47) $\mathbf{w}$ can be regarded as a standard additive disturbance. Then, in Section IV-C problem (47) with the revisited wind model is solved by means of a randomized approach for computational reasons. Eventually, Section IV-D discusses the numerical implementation of the final optimization program so as to further speed up its resolution.

B. Modelling wind in the optimization problem

Both the forecast that provides the wind deterministic component, and the random field that models the wind stochastic component introduce a nonlinear dependence of the wind velocity on the aircraft position (x_1, x_2, x_3), which compromises the convexity of the optimization problem (47). Indeed, the wind forecast is a look-up table that maps the aircraft position into the wind velocities, and the covariance matrices that define the wind random field in (8) depend on the position of the aircraft as well. Note however that, being performed over a finite horizon, optimization at each time step requires the model of the wind over a neighborhood of the current aircraft position only. Since both the deterministic and stochastic components typically show a weak variability in space, the idea is then to build an approximated local model of the wind that does not depend on x_1, x_2 and x_3. This model is updated at each time step so as to track the aircraft change of position in accordance to the receding horizon implementation of the controller.

As for the deterministic component of the wind $\mathbf{w}_{f,k+i}(x_{1,k+i}, x_{2,k+i}, x_{3,k+i})$, $i = 0,\dots,M$, we simply approximate it with $\hat{\mathbf{w}}_{f,k+i}$ which is, i by i, the average of the forecast wind over the hyper-rectangle: $[-V_kT_s, V_kMT_s]\times [-V_kT_s\frac{M}{2}, V_kT_s\frac{M}{2}] \times [V_kT_sM\sin\gamma_{min}, V_kT_sM\sin\gamma_{max}]$, where the origin is centred in the current aircraft position $x_{1,k+i}$, $x_{2,k+i}$, $x_{3,k+i}$ and axes are oriented according to the current aircraft velocity orientation given by ψ_{k+i}, γ_{k+i}. Note that the size of the hyper-rectangle is determined by the amount of space that the aircraft can cover in the finite horizon M according to the current TAS V_k. $\hat{\mathbf{w}}_{f,k+i}$ is computed by gridding the hyper-rectangle, calculating the wind deterministic components in correspondence of these grid points by linear interpolating the data provided by wind forecast and, eventually, by averaging these values. This way $\hat{\mathbf{w}}_{f,k+i}$ is a function of time only and it is straightforward to account for it in the optimization problem. Despite its simplicity, this approach works fine thanks to the limited variability of the wind forecast over the distances traveled in the considered finite prediction horizon.

As for the stochastic component of the wind, $\mathbf{w}_{s,k+i}(x_{1,k+i}, x_{2,k+i}, x_{3,k+i})$, $i = 0,\dots,M$, we approximate it by means of three discrete time stochastic Auto-Regressive (AR) processes, whose parameters are identified based on the past wind values experienced along the aircraft trajectory up to time instant $k-1$ preceding the current time instant k. As a matter of fact, past wind velocities along the aircraft trajectory are easily recovered from the aircraft dynamics in (16) as:

$$\begin{bmatrix} w_{x,l} \\ w_{y,l} \\ w_{z,l} \end{bmatrix} = \frac{1}{T_s}\left(\begin{bmatrix} x_{1,l+1} \\ x_{2,l+1} \\ x_{3,l+1} \end{bmatrix} - \begin{bmatrix} x_{1,l} \\ x_{2,l} \\ x_{3,l} \end{bmatrix}\right) - \begin{bmatrix} x_{4,l} \\ x_{5,l} \\ x_{6,l} \end{bmatrix} - \frac{T_s}{2}\begin{bmatrix} u_{1,l} \\ u_{2,l} \\ u_{3,l} \end{bmatrix}, \tag{48}$$

from which the past stochastic wind components can be computed by simply subtracting the deterministic ones. The computed values $w_{xs,l}$, $w_{ys,l}$, $w_{zs,l}$, $l = 0,1,\dots,k-1$, are seen as realizations of time series and used to recursively identify the following AR models, one for each wind stochastic component:

$$\begin{aligned} \hat{w}_{xs,l} &= \varphi_{xs,l}^T\theta_x + e_{xs,l} \\ \hat{w}_{ys,l} &= \varphi_{ys,l}^T\theta_y + e_{ys,l} \\ \hat{w}_{zs,l} &= \varphi_{zs,l}^T\theta_z + e_{zs,l} \end{aligned} \tag{49}$$

where $e_{xs} \sim WGN(0,\lambda_x^2)$, $e_{ys} \sim WGN(0,\lambda_y^2)$, $e_{zs} \sim WGN(0,\lambda_z^2)$ (WGN stands for White Gaussian Noise) and

$$\begin{aligned} \varphi_{xs,l} &= [\hat{w}_{xs,l-1},\dots,\hat{w}_{xs,l-m},1]^T \\ \varphi_{ys,l} &= [\hat{w}_{ys,l-1},\dots,\hat{w}_{ys,l-m},1]^T \\ \varphi_{zs,l} &= [\hat{w}_{zs,l-1},\dots,\hat{w}_{zs,l-m},1]^T \end{aligned}$$

are the regressors, m is the model order, and θ_x, θ_y, θ_z are the model parameter vectors. Note that, given the strong wind correlation with respect to both time and space it may be that non zero mean models have to be preferred to best fit the available data records: the ones in the regressors are introduced to this purpose. The identified AR models are used as models for the stochastic wind components over the finite horizon $[k, k+M]$.

Eventually, at each time step, a new data point, computed via (48), becomes available and the AR models have to be updated. To this purpose we resort to the Recursive Least Square (RLS) algorithm with forgetting factor μ:

$$\begin{aligned} \theta_{j,k} &= \theta_{j,k-1} + S_{j,k}\varphi_{js,k-1}(w_{js,k-1} - \varphi_{js,k-1}^T\theta_{j,k-1}) \\ S_{j,k} &= \frac{1}{\mu}(S_{j,k-1} - \frac{S_{j,k-1}\varphi_{js,k-1}\varphi_{js,k-1}^T S_{i,k-1}}{\mu + \varphi_{js,k-1}^T S_{j,k}\varphi_{js,k-1}}) \\ j &= x,y,z. \end{aligned} \tag{50}$$

The white noise variances are also estimated as:

$$\lambda_j^2 = \frac{\sum_{i=1}^{k-1} \mu^{k-i}(w_{js,i} - \varphi_{js,i}^T \theta_{j,k})^2}{\sum_{i=1}^{k-1} \mu^{k-i}}, \quad j = x, y, z.$$

Note that in the AR models the dependence of the wind with respect to space position is neglected. However, thanks to the fact that the identification is repeated at each time step and that a forgetting factor is introduced so as to discard past data that are no more representative of the current situation, the model is tuned to the wind characteristics in the region of space close to the current aircraft position. The strong correlation of the wind in time and space should further foster the identification of a good model for the wind. Note also that the proposed approach can be used irrespectively of the availability of the stochastic model of the wind field in (8). Also it can account for all disturbances other than wind acting on the aircraft model as due to model errors, noisy measurements or noisy reconstructions of the state variables, etc. This way its usage can enforce additional robustness to the design of the controller.

C. Resolution of the optimization problem with the scenario approach

The finite horizon optimization problem (47) can be reformulated as follows by simply replacing $\mathbf{w}$ with $\hat{\mathbf{w}} = \hat{\mathbf{w}}_f + \hat{\mathbf{w}}_s$ as given by the proposed approximate wind model:

$$\min_{\substack{\mathbf{u}_{k+i}\, i=0\dots M-1 \\ h_{L,i},\ h_{l,i},\ h_{v,i}\, i=1\dots M}} J \text{ subject to:} \tag{51}$$

constraints (31) (32) (34) (35) (39) (41) (44)

$$\mathbb{P}\{|\xi_{k+i}(\hat{\mathbf{w}}_k, \dots, \hat{\mathbf{w}}_{k+i-1})| \le \begin{bmatrix} h_{L,i} \\ h_{l,i} \\ h_{v,i} \end{bmatrix}, i = 1, \dots, M\} \ge 1 - \varepsilon.$$

Being $\hat{\mathbf{w}}_l$ a Gaussian process that enters additively the state equation and that is independent of the input $\mathbf{u}_{k+i}$, $i = 1, \dots, M$, it can be proved that the probabilistic constraint in (51) is indeed a convex constraint, see [33], [34]. Nonetheless the resolution of (51) may still be problematic because the obtained constraint does not belong in general to classes of constraints for which efficient resolution algorithms exist, and general purpose algorithms have to be used instead. This drawback is particularly annoying in the present aircraft motion control application because problem (51) is meant to be solved on board in a small fraction of the sampling time with limited computational resources.

We, hence, resort to the scenario approach, a randomized method to approximately solve chance-constrained problems such as (51), which has been recently introduced and discussed in [22], [23] and applied to stochastic constrained control and receding horizon control in [26], [19], [27], [35], [25]. The idea of the scenario approach is very simple: a bunch of N realizations of the disturbance, say $\{\hat{\mathbf{w}}_k^{(j)}\ \hat{\mathbf{w}}_{k+1}^{(j)}\ \dots \hat{\mathbf{w}}_{k+M-1}^{(j)}\}$, $j = 1, \dots, N$, are generated according to the last identified model for wind, where the last m wind observations $\mathbf{w}_{k-1}$,…,$\mathbf{w}_{k-m}$ are used as initialization of (49). Then, the probabilistic constraint is replaced with the N constraints obtained in correspondence of the extracted disturbance realizations. Namely:

$$\min_{\substack{\mathbf{u}_{k+i}\, i=0\dots M-1 \\ h_{L,i},\ h_{l,i},\ h_{v,i}\, i=1\dots M}} J \text{ subject to:} \tag{52}$$

constraint (31) (32) (34) (35) (39) (41) (44)

$$|\xi_{k+i}(\hat{\mathbf{w}}_k^{(j)}, \dots, \hat{\mathbf{w}}_{k+i-1}^{(j)})| \le \begin{bmatrix} h_{L,i} \\ h_{l,i} \\ h_{v,i} \end{bmatrix},$$

$$i = 1, \dots, M,\ j = 1, \dots, N.$$

Note that the new N constraints replacing the probabilistic one are linear constraints, and, overall, (52) is a quadratically constrained quadratic program which can be very efficiently solved by means of standard solver like e.g. CPLEX, [36]. Moreover, despite its apparent naivety the scenario approach is grounded on a solid theory that provides precise guarantees about the feasibility of the solution obtained solving problem (52) for the original chance-constrained problem (51).

More precisely, according to the results of [24] along with the explicit expression for N provided in [37], [38], if N is chosen so as to satisfy

$$N \ge \frac{1}{\epsilon}\left(d + 1 + \ln(1/\beta) + \sqrt{2(d+1)\ln(1/\beta)}\right), \tag{53}$$

where d is the number of optimization variables (in our setup $d = 6M$), then the solution of problem (52) is feasible for problem (51) with confidence $1-\beta$. Thanks to the logarithmic dependence, very small values of β such as 10^{-6} or even 10^{-9} can be enforced without affecting N too much, and, with such small values for β, the solution achieved solving (52) can be deemed feasible for (51) beyond any reasonable doubts.

The guarantee inherited from the results of [24] described above regards the solution of each finite horizon optimization problem (52). In the receding horizon implementation, the solution is recomputed at each time step by shifting the time horizon one step forward, and one is typically interested in evaluating the behavior of the resulting closed-loop control system. To this purpose, let $(\mathbf{u}_k^\star, h_{L,k+1}^\star, h_{l,k+1}^\star, h_{v,k+1}^\star)$ be that part of the solution of problem (52) that refers to the first-time-instant and, hence, provides the input that, k by k, is actually applied to the aircraft system, according to the receding horizon implementation. Denote by $\mathbf{x}_{k+1}^\star$ and $\xi_{k+1}^\star$ the corresponding closed loop aircraft state and position error respectively. Constraints (31), (32), (34), (35), (39), (41), (44) are satisfied by $\mathbf{u}_k^\star$, $\mathbf{x}_{k+1}^\star$ by construction, and, hence, the original physical and comfort limitations posed in (2)-(7) are met for every k.

Let

$$v_k = \begin{cases} 1 & \text{if } \xi_k^\star \le [h_{L,k}^\star, h_{l,k}^\star, h_{v,k}^\star]^T \\ 0 & \text{otherwise} \end{cases}.$$

Consider the condition

$$\lim_{k\to\infty} \inf \frac{1}{k} \sum_{j=0}^{k} v_j \ge 1 - \epsilon, \tag{54}$$

i.e., that the ratio of the number of times in which the actual position error $\xi_k^\star$ is within the bounds $h_{L,k}^\star$, $h_{l,k}^\star$, $h_{v,k}^\star$ is asymptotically larger than or equal to $1-\epsilon$. A specific analysis

tailored to the problem of evaluating this asymptotic ratio (see [39], [27]) shows that

$$\lim_{k\to\infty} \inf \frac{1}{k}\sum_{j=0}^{k} v_j \geq 1 - \frac{d}{N+1} \tag{55}$$

almost surely, and, hence, it is enough to take N in (52) such that

$$N \geq \frac{d}{\varepsilon} - 1, \tag{56}$$

with a reduction of the disturbance extractions required at each time k. Given that only the satisfaction of thresholds $h^{\star}_{L,k}$, $h^{\star}_{l,k}$, $h^{\star}_{v,k}$ at the current time k enters the definition of v_k, it is more convenient to reformulate the scenario program (52) as follows

$$\begin{aligned}
&\min_{\substack{\mathbf{u}_{k+i}\ i=0\dots M-1\\ h_{L,i},\ h_{l,i},\ h_{v,i}\ i=1\dots M}} J \text{ subject to:} \qquad (57)\\
&\text{constraint (31) (32) (34) (35) (39) (41) (44)}\\
&|\xi_{k+1}(\hat{\mathbf{w}}_k^{(j)})| \leq \begin{bmatrix} h_{L,1}\\ h_{l,1}\\ h_{v,1}\end{bmatrix},\ j = 1\dots N\\
&|\xi_{k+i}(\hat{\mathbf{w}}_k^{(j')},\dots,\hat{\mathbf{w}}_{k+i-1}^{(j')})| \leq [\begin{bmatrix} h_{L,i}\\ h_{l,i}\\ h_{v,i}\end{bmatrix},\\
&i = 2,\dots,M,\ j' = N+1,\dots,N+N',
\end{aligned}$$

where the first time instant position error constraint is accounted for separately from the constraint corresponding to the other time steps, and $N+N'$ extractions of $\hat{\mathbf{w}}$ are considered. In this case, extractions $N+1,\dots,N+N'$ play no role as for guaranteeing (54), and, hence, N' can be decided separately, either heuristically or in order to obtain $\mathbb{P}\{|\xi_{k+i}(\hat{\mathbf{w}}_k,\dots,\hat{\mathbf{w}}_{k+i-1})| \leq [h_{L,i}\ h_{l,i}\ h_{v,i}]^T\} \geq 1-\epsilon'$ for some $\epsilon' \geq \epsilon$, using the bound (53) with d replaced by $6M-6$ and ϵ by ϵ'. Correspondingly, (55) becomes

$$\lim_{k\to\infty} \inf \frac{1}{k}\sum_{j=0}^{k} v_j \geq 1 - \frac{\zeta}{N+1},$$

where ζ is the number of optimization variables appearing in the first-time-instant constraint only (in the case at hand $\zeta = 6$), and, hence, condition (56) can be rewritten as:

$$N \geq \frac{\zeta}{\varepsilon} - 1, \tag{58}$$

which further reduces the number of required disturbance realizations, and hence the computational effort.

D. Numerical issues

The scenario problems (52) and (57) can be very efficiently solved thanks to their particular structure and to convexity.

By accounting for the system dynamics (16), the position constraints in these problems can be rewritten as:

$$\begin{aligned}
&\left| R_z(\psi^R_{k+i}) \left(\begin{bmatrix} x_{1,k} + T_s \sum_{l=0}^{i-1} x_{4,k+l}(u_1) + \frac{T_s^2}{2}\sum_{l=0}^{i-1} u_{1,k+l}\\ x_{2,k} + T_s \sum_{l=0}^{i-1} x_{5,k+l}(u_2) + \frac{T_s^2}{2}\sum_{l=0}^{i-1} u_{2,k+l}\\ x_{3,k} + T_s \sum_{l=0}^{i-1} x_{6,k+l}(u_3) + \frac{T_s^2}{2}\sum_{l=0}^{i-1} u_{3,k+l}\end{bmatrix} \right.\right.\\
&\left.\left. + T_s \begin{bmatrix} \sum_{l=0}^{i-1} w^{(j)}_{x,k+l}\\ \sum_{l=0}^{i-1} w^{(j)}_{y,k+l}\\ \sum_{l=0}^{i-1} w^{(j)}_{z,k+l}\end{bmatrix} - \begin{bmatrix} x^R_{1,k+i}\\ x^R_{2,k+i}\\ x^R_{3,k+i}\end{bmatrix} \right) \right| \leq \begin{bmatrix} h_{L,k+i}\\ h_{l,k+i}\\ h_{v,k+i}\end{bmatrix}. \qquad (59)
\end{aligned}$$

We can then isolate in each row the term that depends on the wind disturbance, and consider the constraints that correspond to the worst case among the extracted wind realizations, in place of all the constraints. That is the position constraints (61) are equivalent to:

$$\begin{aligned}
&- \begin{bmatrix} h_{L,k+i}\\ h_{l,k+i}\\ h_{v,k+i}\end{bmatrix} - \min_{j=1,\dots,N} \left\{ R_z(\psi^R_{k+i}) T_s \begin{bmatrix} \sum_{l=0}^{i-1} w^{(j)}_{x,k+l}\\ \sum_{l=0}^{i-1} w^{(j)}_{y,k+l}\\ \sum_{l=0}^{i-1} w^{(j)}_{z,k+l}\end{bmatrix} \right\}\\
&\leq R_z(\psi^R_{k+i}) \left(- \begin{bmatrix} x^R_{1,k+i}\\ x^R_{2,k+i}\\ x^R_{3,k+i}\end{bmatrix} \right. \qquad (60)\\
&\left. + \begin{bmatrix} x_{1,k} + T_s \sum_{l=0}^{i-1} x_{4,k+l}(u_1) + \frac{T_s^2}{2}\sum_{l=0}^{i-1} u_{1,k+l}\\ x_{2,k} + T_s \sum_{l=0}^{i-1} x_{5,k+l}(u_2) + \frac{T_s^2}{2}\sum_{l=0}^{i-1} u_{2,k+l}\\ x_{3,k} + T_s \sum_{l=0}^{i-1} x_{6,k+l}(u_3) + \frac{T_s^2}{2}\sum_{l=0}^{i-1} u_{3,k+l}\end{bmatrix} \right)\\
&\leq \begin{bmatrix} h_{L,k+i}\\ h_{l,k+i}\\ h_{v,k+i}\end{bmatrix} - \max_{j=1,\dots,N} \left\{ R_z(\psi^R_{k+i}) T_s \begin{bmatrix} \sum_{l=0}^{i-1} w^{(j)}_{x,k+l}\\ \sum_{l=0}^{i-1} w^{(j)}_{y,k+l}\\ \sum_{l=0}^{i-1} w^{(j)}_{z,k+l}\end{bmatrix} \right\},
\end{aligned}$$

By accounting for the system dynamics (16), the position constraints in these problems can be rewritten as:

$$\begin{aligned}
&\left| R_z(\psi^R_{k+i}) \left(\begin{bmatrix} x_{1,k} + T_s \sum_{l=0}^{i-1} x_{4,k+l}(u_1) + \frac{T_s^2}{2}\sum_{l=0}^{i-1} u_{1,k+l}\\ x_{2,k} + T_s \sum_{l=0}^{i-1} x_{5,k+l}(u_2) + \frac{T_s^2}{2}\sum_{l=0}^{i-1} u_{2,k+l}\\ x_{3,k} + T_s \sum_{l=0}^{i-1} x_{6,k+l}(u_3) + \frac{T_s^2}{2}\sum_{l=0}^{i-1} u_{3,k+l}\end{bmatrix} \right.\right.\\
&\left.\left. + T_s \begin{bmatrix} \sum_{l=0}^{i-1} w^{(j)}_{x,k+l}\\ \sum_{l=0}^{i-1} w^{(j)}_{y,k+l}\\ \sum_{l=0}^{i-1} w^{(j)}_{z,k+l}\end{bmatrix} - \begin{bmatrix} x^R_{1,k+i}\\ x^R_{2,k+i}\\ x^R_{3,k+i}\end{bmatrix} \right) \right| \leq \begin{bmatrix} h_{L,k+i}\\ h_{l,k+i}\\ h_{v,k+i}\end{bmatrix}. \qquad (61)
\end{aligned}$$

We can then isolate in each row the term that depends on the wind disturbance, and consider the constraints that correspond to the worst case among the extracted wind realizations, in place of all the constraints. That is the position constraints (61) are equivalent to:

$$\begin{aligned}
&- \begin{bmatrix} h_{L,k+i}\\ h_{l,k+i}\\ h_{v,k+i}\end{bmatrix} - \min_{j=1,\dots,N} \left\{ R_z(\psi^R_{k+i}) T_s \begin{bmatrix} \sum_{l=0}^{i-1} w^{(j)}_{x,k+l}\\ \sum_{l=0}^{i-1} w^{(j)}_{y,k+l}\\ \sum_{l=0}^{i-1} w^{(j)}_{z,k+l}\end{bmatrix} \right\}\\
&\leq R_z(\psi^R_{k+i}) \left(- \begin{bmatrix} x^R_{1,k+i}\\ x^R_{2,k+i}\\ x^R_{3,k+i}\end{bmatrix} \right. \qquad (62)\\
&\left. + \begin{bmatrix} x_{1,k} + T_s \sum_{l=0}^{i-1} x_{4,k+l}(u_1) + \frac{T_s^2}{2}\sum_{l=0}^{i-1} u_{1,k+l}\\ x_{2,k} + T_s \sum_{l=0}^{i-1} x_{5,k+l}(u_2) + \frac{T_s^2}{2}\sum_{l=0}^{i-1} u_{2,k+l}\\ x_{3,k} + T_s \sum_{l=0}^{i-1} x_{6,k+l}(u_3) + \frac{T_s^2}{2}\sum_{l=0}^{i-1} u_{3,k+l}\end{bmatrix} \right)\\
&\leq \begin{bmatrix} h_{L,k+i}\\ h_{l,k+i}\\ h_{v,k+i}\end{bmatrix} - \max_{j=1,\dots,N} \left\{ R_z(\psi^R_{k+i}) T_s \begin{bmatrix} \sum_{l=0}^{i-1} w^{(j)}_{x,k+l}\\ \sum_{l=0}^{i-1} w^{(j)}_{y,k+l}\\ \sum_{l=0}^{i-1} w^{(j)}_{z,k+l}\end{bmatrix} \right\},
\end{aligned}$$

where min and max have to be computed row-wise. The computation of these minimum and maximum values is extremely straightforward and the resulting convex optimization problem obtained replacing in (52) or (57) the position constraints with the formulation in (62) can be solved at very low computational effort.

E. Final remarks on the receding horizon control strategy

It is worth noticing that we are computing at each time step k an open loop control law consisting of M values $\mathbf{u}_k, \ldots, \mathbf{u}_{k+M-1}$ for the control input by solving the optimization problem (47), which contains a probabilistic constraint due to the presence of the stochastic wind. As a result, $\mathbf{u}_k, \ldots, \mathbf{u}_{k+M-1}$ will depend on the stochastic wind characteristics. Only $\mathbf{u}_k$ will be applied and computation of $\mathbf{u}_{k+1}$ will be performed at $k+1$ by solving the same kind of optimization problem but with an updated probabilistic constraint since the wind model is identified on-line and updated at each time step (see Section IV-B). As a result of the receding horizon implementation, the applied control input will depend on the stochastic wind field actually experienced by the aircraft for a twofold reason: wind affects the aircraft state and the wind model adopted for control design is identified on-line based on state measurements.

V. Numerical results

In this section, we report some numerical results obtained from simulations in which the proposed receding horizon control strategy is applied to a 4-D trajectory tracking problem. The reference 4-D trajectory is computed as in [11], hence, it is feasible in nominal conditions.

Our aim is to evaluate the capability of the control strategy to steer the aircraft and keep it close to the reference 4-D trajectory while counteracting the action of the wind. We also verify that the introduced approximation of the constraints do not adversely affect the solution.

In the simulations, we suppose that the aircraft starts at the beginning of the reference trajectory, namely $\mathbf{x}_0 = [-60 \; -6 \; 6 \; 600 \; 600 \; 0]^T$ (positions are in km, velocities in km/h) and perform 900 steps with a sample time $T_s = 2$s. We set the prediction horizon $M = 20$, and the weights in the cost function (46) equal to $R_c = \text{diag}(0.125,\ 1,\ 0.25)$, $\mu_{ld} = 0.72$, $\mu_{Lc} = 8$, $\mu_{lc} = 6$, $\mu_{vc} = 6$, $\mu_{ud} = 0.72$, $\mu_{Ld} = 0.72$, $\mu_{vd} = 0.72$.

Simulations are run by applying to the original nonlinear model of the aircraft (1) (with the mass dynamics neglected) the original control inputs (AoA, bank angle, and engine thrust) as derived from the designed new inputs (Cartesian components of the aircraft acceleration with respect to the air) through the state feedback linearizing control law in Section III.

We adopt the formulation in (57), where $N = 59$ is chosen according to (58) with $\varepsilon = 0.1$. N' is set equal to N.

The system parameters and the bounds for the constraints on physical limitations and passenger comfort are set as follow: $V_{max} = 910$ km/h, $V_{min} = 600$ km/h, $T_{max} = 2 \cdot 276$ kN, $T_{min} = T_{max}/200$, $\bar{\phi} = 40°$, $\gamma_{max} = 5°$, $\gamma_{min} = -3°$, $a_L = 2$ ft/s^2 $= 0.6$ m/s^2, $a_Z = 5$ ft/s^2 $= 1.5$ m/s^2, $m = 150\ 10^3$ kg, $S = 0.28\ 10^3$ m^2, $C_d = 0.026$, $C_l = 0.24$, $b_1 = 12.6$, $b_2 = 377$, $a = 59$. The stochastic wind random field parameters are set as: $\sigma_1 = 6\ 10^{-4}$, $\sigma_2 = 1.6\ 10^{-5}$, $\sigma_3 = 1.5\ 10^{-4}$, $k(z) = \frac{z}{3} + 5$, $\sigma_{1z} = 6\ 10^{-4}$, $\sigma_{2z} = 1.5\ 10^{-4}$, $\sigma_{3z} = 1.6\ 10^{-5}$, $k_z(z) = 0.5(\frac{z}{3} + 5)$.

Simulation results are reported in Figure 1, where a 3-D view of the actual trajectory of the aircraft, along with the reference trajectory, is depicted.

The control strategy has been implemented in MATLAB equipped with an IBM ILOG CPLEX solver, [36], running on a desktop pc with two Intel Xeon E5-2630 2.30 GHz processors and 64Gb of RAM: the resolution of the optimization problem with a finite horizon $M = 20$ requires about 0.3 s. The computational time can be further reduced by means of an embedded implementation and problem-specific solvers, such as FORCES, [40].

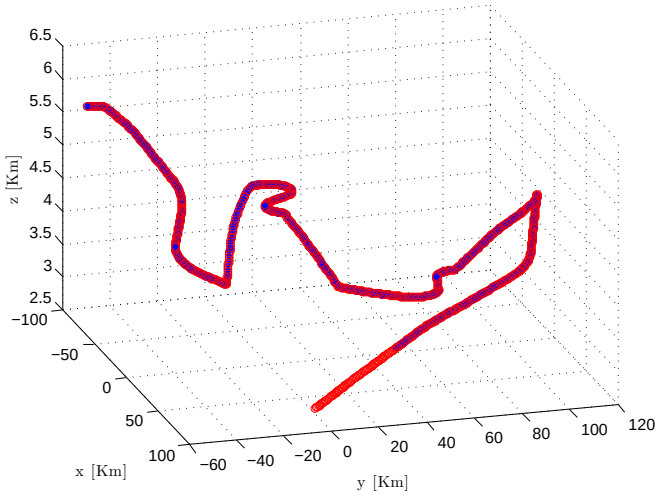

Fig. 1: Aircraft trajectory: receding horizon solution (blue stars) and reference trajectory (red circle).

In Figure 2, the finite horizon solution computed at each step is plotted together with the receding horizon solution and the reference trajectory. The reference trajectory is well tracked by the aircraft, and, moreover, the original constraints are satisfied all along the aircraft trajectory. Though the approximation introduced to attain convexity hampers the finite horizon solutions to make fast turn, it appears that this approximation does not adversely affect the actual behavior of the aircraft, thanks to the beneficial effect of the receding horizon implementation.

In Figure 3 the values for $h^\star_{L,k}$, $h^\star_{l,k}$, and $h^\star_{v,k}$ are reported together with the position error $|\xi_k|$. As one can see, the position error keeps almost always below 100 m and it is usually even smaller especially on the normal and vertical components. The computed bounds $h^\star_{L,k}$, $h^\star_{l,k}$, and $h^\star_{v,k}$ are quite close to the actual position error: it results that the first step position constraint is violated, namely $|\xi_k|$ is greater than the corresponding bound $[h^\star_{L,k}\ h^\star_{l,k}\ h^\star_{v,k}]$ computed at time $k-1$, only for 5.2% of the steps.

In Figure 4 the actual wind values along the aircraft trajectory are reported, together with some of the wind sample

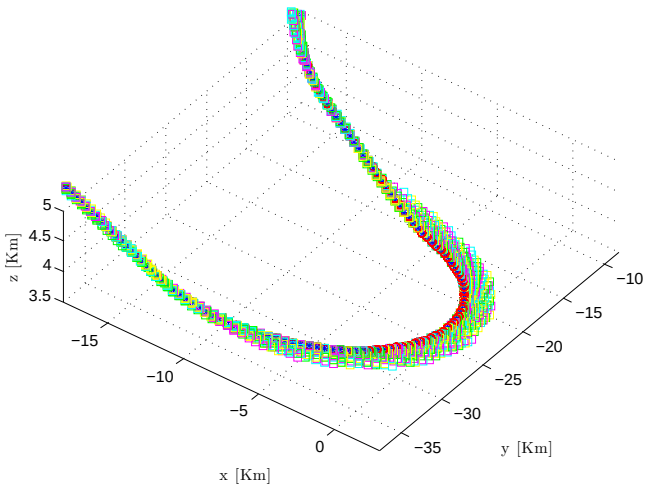

Fig. 2: Aircraft trajectory: receding horizon solution (blue stars) and reference trajectory (red circle) together with the finite horizon solutions obtained at each time step (colored squares).

realizations used in the solution of the finite horizon optimization problems. The wind samples are obtained by simulation of the three recursively identified 3^{rd}-order AR models, as described in Section IV-B, while the actual wind encountered by the aircraft is generated according to the forecast and to the random field as described in Section II-B.

We also run a simulation where wind acts on the aircraft but it is not accounted for when computing the receding horizon control strategy, namely $\mathbf{w}$ is set equal to zero in the finite horizon optimization problem. The resulting position error ξ is compared with the one obtained by accounting for the wind in Figure 5. The position error obtained without accounting for the wind is greater than the one obtained accounting for the wind presence in the optimization problem. Quantitatively. the sum along the time horizon of length 900 of the absolute value of the error in the three spatial coordinates is [60.47 27.40 7.80] versus [8.74 2.98 0.93].

Note that Figures 1–5 refer to a single wind realization, but they are in fact representative of the behavior observed in multiple runs of the algorithm. To better validate our approach, we next compute a bound on the position error that is guaranteed to hold along the whole trajectory with high probability with respect to the wind realizations. We also determine the probability distribution of the largest position error over the whole trajectory as obtained via multiple runs with different wind realizations.

A. Validation

By means of the proposed approach, we find bounds h_L, h_l, h_v on the position error ξ that change at every time step, and that, of course, depend on the particular wind realization used in the simulation. Our aim is to validate the performance of the controller finding a bound h_p on the position error that is guaranteed to hold along the whole considered trajectory with high probability with respect to the wind realizations.

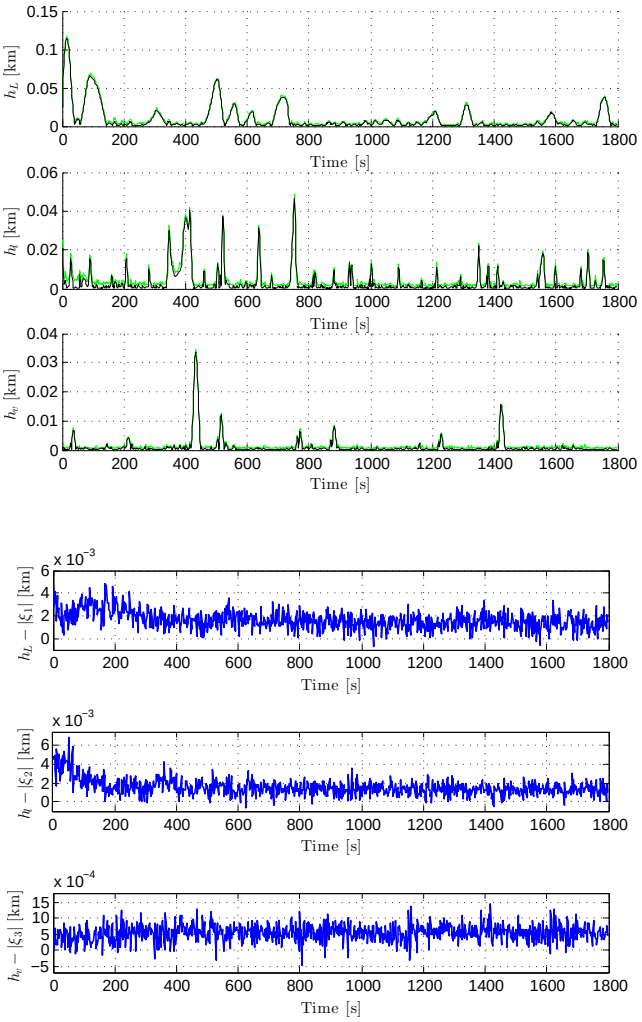

Fig. 3: Absolute value of the aircraft position error ξ_k in black and $h^\star_{L,k}$, $h^\star_{l,k}$, $h^\star_{v,k}$ in green (top plots) and corresponding differences (bottom plots).

The computation of such a bound h_p can be addressed by means of a chance-constrained optimization problem:

$$\min_{h_p} h_p \text{ subject to:} \qquad (63)$$
$$\mathbb{P}\{\max_k \|\xi_k(\mathbf{w})\|_2 \leq h_p\} \geq 1 - \varepsilon_v.$$

The value of h_p achieved solving (63) represents a probabilistic bound on the maximal distance between aircraft position and reference trajectory. Problem (63) can be solved again using the scenario theory: the bound h_p can be computed simply performing N_p simulations in which the aircraft is controlled by means of the developed controller applied in a receding horizon fashion for a given reference trajectory, considering different wind realizations. Then we take $h_p = \max_{j=1\ldots N_p}\{\max_k \|\xi_k(\mathbf{w})\|_2^{(j)}\}$. The number N_p of simulations should be chosen according to (53) to achieve the desired probabilistic guarantees for the obtained bound h_p.
For the computation of the probabilistic bound h_p, we set

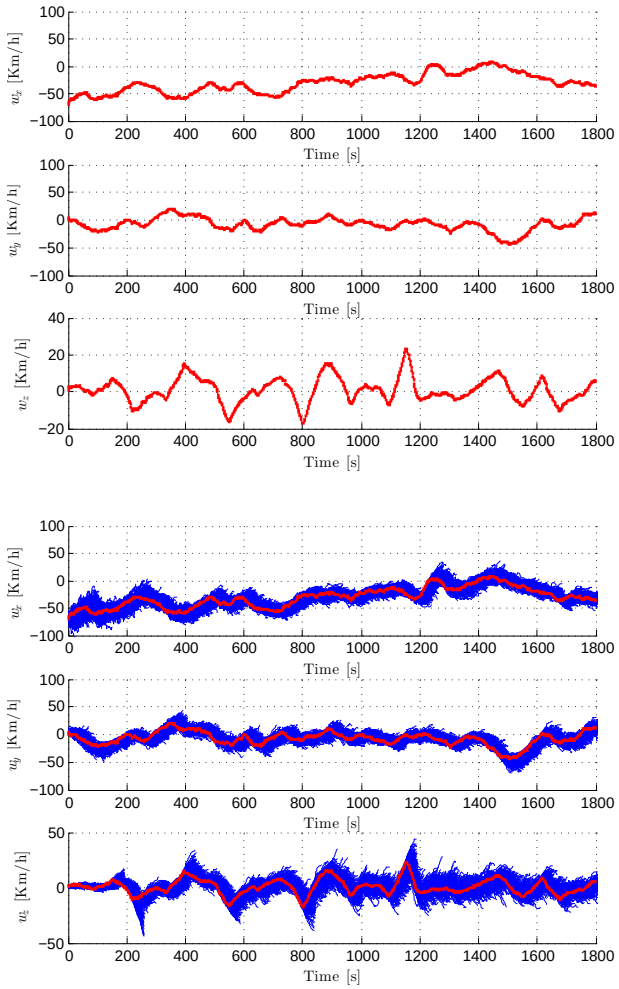

Fig. 4: Actual wind components along the aircraft trajectory on their own (top plots) and together with 10 samples generated at each time step from the latest identified AR models (bottom plots).

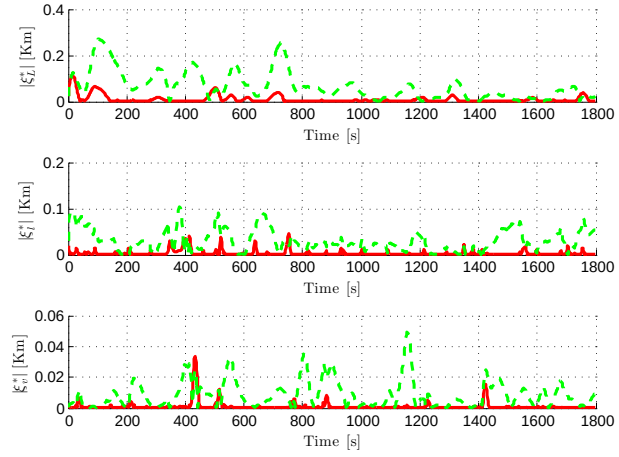

Fig. 5: Absolute value of the position error ξ obtained accounting for the wind (red solid line) and neglecting it (green dashed line) in the finite horizon optimization problem.

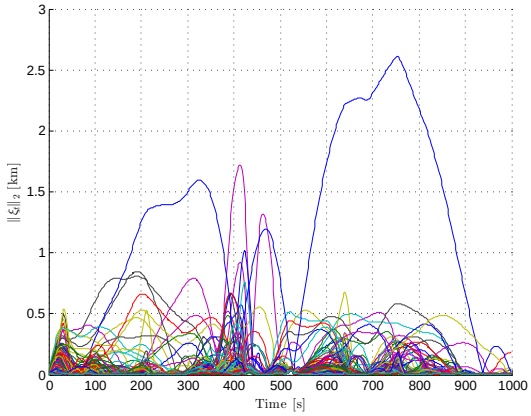

(a) Behavior of $\|\xi_k\|_2$ corresponding to different wind disturbance realizations.

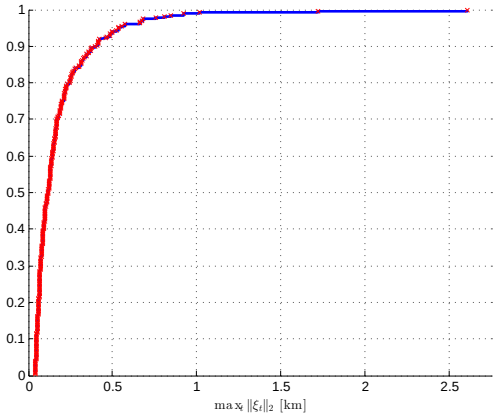

(b) Sampled distribution of $\max_k \|\xi_k\|_2$ obtained from simulations with different wind disturbance.

Fig. 6: Validation of the proposed strategy.

$\varepsilon_p = 0.05$, and $\beta = 10^{-6}$ so that it results $N_p = 270$. Figure 6(a) plots $\|\xi_k(\mathbf{w})\|_2$ obtained for different simulations of 500 steps, using the same values of the parameters described above. In most of the simulations, the position error keeps much below the bound h_p that is equal to 2.6 km. This is clear from the obtained sampled distribution of $\max_k \|\xi_k\|_2$ reported in Figure 6(b).

VI. Conclusion

In this paper, we have developed a receding horizon control strategy for an aircraft to automatically track a 4-D reference trajectory. Constraints arising from physical limitations and comfort requirements are explicitly accounted for while steering the aircraft along the reference trajectory and counteracting the action of the wind. The proposed approach integrates feedback linearization and scenario optimization within a receding horizon framework, which allows for achieving recursive feasibility and designing a control action better tailored to the uncertainty affecting the aircraft motion via on-line identification. Note that the on-line identification of the wind disturbance model allows to account also for parametric uncertainty and

unmodeled dynamics, thus coping with the robustness issue that is typically affecting feedback linearization, which is based on an exact cancelation of the system nonlinearities. The interested reader is referred to [11] where robustness of the designed control strategy with respect to mass uncertainty is studied and proved through intensive experiments.

The proposed approach has some potential for application within emerging novel operational paradigms in air traffic management based on 4-D trajectory and the concept of target windows.

REFERENCES

[1] CATS - Contract based Air Transportation System Project, "Deliverable D1.1," http://www.cats-fp6.aero/public_deliverables.html, June 2008.

[2] ——, "Deliverable D2.2.4.3," http://www.cats-fp6.aero/public_deliverables.html, October 2010.

[3] B. Schwartz and S. Benjamin, "A comparison of temperature and wind measurements from acars-equipped aircraft and rawinsondes," *Weather and forecasting*, vol. 10, no. 3, pp. 528–544, 1995.

[4] S. Benjamin, B. Schwartz, and R. Cole, "Accuracy of acars wind and temperature observations determined by collocation." *Weather & Forecasting*, vol. 14, no. 6, 1999.

[5] S. Benjamin, B. Schwartz, E. Szoke, and S. Koch, "The value of wind profiler data in us weather forecasting." *Bulletin of the American Meteorological Society*, vol. 85, no. 12, 2004.

[6] J. Hu, M. Prandini, and S. Sastry, "Aircraft conflict prediction in presence of a spatially correlated wind field," *IEEE Transactions on Intelligent Transportation Systems*, vol. 6, no. 3, pp. 326–340, 2005.

[7] G. Chaloulos and J. Lygeros, "Effect of Wind Correlation on Aircraft Conflict Probability," *AIAA Journal of Guidance, Control, and Dynamics*, vol. 30, no. 6, pp. 1742–1752, 2007.

[8] W. Glover and J. Lygeros, "A stochastic hybrid model for air traffic control simulation," in *Hybrid Systems: Computation and Control*. Springer, 2004, pp. 372–386.

[9] I. Lymperopoulos, J. Lygeros, A. L. Visintini, J. M. Maciejowski, and W. Glover, "A Stochastic Hybrid Model for Air Traffic Management Processes," Cambridge, Tech. Rep., 2007.

[10] I. Lymperopoulos, "Sequential Monte Carlo methods in air traffic management," Ph.D. dissertation, Diss., Eidgenössische Technische Hochschule ETH Zürich, Nr. 19004, 2010, 2010.

[11] L. Deori, "A model predictive control approach to aircraft motion control," Ph.D. dissertation, Politecnico di Milano, Milano, Italy, 2015.

[12] R. Patel and P. Goulart, "Trajectory generation for aircraft avoidance maneuvers using online optimization," *Journal of guidance, control, and dynamics*, vol. 34, no. 1, pp. 218–230, 2011.

[13] M. Kurtz and M. Henson, "Input-output linearizing control of constrained nonlinear process," *Journal of Process Control*, vol. 7, no. 1, pp. 3–17, 1997.

[14] W. Van Soest, Q. Chu, and J. Mulder, "Combined feedback linearization and constrained model predictive control for entry flight," *Journal of Guidance, Control, and Dynamics*, vol. 29, no. 2, pp. 427–434, 2006.

[15] D. Joosten, T. van den Boom, and T. Lombaerts, "Computationally efficient use of MPC and dynamic inversion for reconfigurable flight control," in *AIAA Guidance, Navigation and Control Conference and Exhibit*, Hawaii, August 2008.

[16] D. Simon, J. Löfberg, and T. Glad, "Nonlinear model predictive control using feedback linearization and local inner convex constraint approximations," in *2013 European Control Conference*, 2013, pp. 2056–2061.

[17] NOAA, "Rapid refresh," http://rapidrefresh.noaa.gov/.

[18] W. Glover and J. Lygeros, "A multi-aircraft model for conflict detection and resolution algorithm evaluation," *HYBRIDGE Deliverable D1.3*, 2004.

[19] L. Deori, S. Garatti, and M. Prandini, "Stochastic constrained control: trading performance for state constraint feasibility," in *2013 European Control Conference*, 2013.

[20] ——, "Stochastic control with input and state constraints: a relaxation technique to ensure feasibility," in *54th IEEE Conference on Decision and Control*, 2015.

[21] ——, "Trading performance for state constraint feasibility in stochastic constrained control: A randomized approach," *Journal of the Franklin Institute*, vol. 354, no. 1, pp. 501 – 529, 2017.

[22] G. Calafiore and M. Campi, "Uncertain convex programs: randomized solutions and confidence levels," *Mathematical Programming*, vol. 102, no. 1, pp. 25–46, 2005.

[23] ——, "The scenario approach to robust control design," *IEEE Transactions on Automatic Control*, vol. 51, no. 5, pp. 742–753, 2006.

[24] M. Campi and S. Garatti, "The exact feasibility of randomized solutions of uncertain convex programs," *SIAM Journal on Optimization*, vol. 19, no. 3, pp. 1211–1230, 2008.

[25] M. Campi, S. Garatti, and M. Prandini, "The scenario approach for systems and control design," *Annual Reviews in Control*, vol. 33, no. 2, pp. 149–157, 2009.

[26] M. Prandini, S. Garatti, and J. Lygeros, "A randomized approach to stochastic model predictive control," in *51st IEEE Conference on Decision and Control*, 2012, pp. 7315–7320.

[27] G. Schildbach, L. Fagiano, C. Frei, and M. Morari, "The scenario approach for stochastic model predictive control with bounds on closed-loop constraint violations," *Automatica*, vol. 50, no. 12, pp. 3009–3018, 2014.

[28] L. Deori, S. Garatti, and M. Prandini, "A model predictive control approach to aircraft motion control," in *2015 American Control Conference*, July 2015, pp. 2299–2304.

[29] ——, "A stochastic strategy integrating wind compensation for trajectory tracking in aircraft motion control," in *2016 IEEE 55th Conference on Decision and Control*, Dec 2016, pp. 256–261.

[30] K. P. Bollino, "High-fidelity real-time trajectory optimization for reusable launch vehicles," Ph.D. dissertation, Naval Postgraduate School, Monterey, California, 2006.

[31] K. Margellos and J. Lygeros, "Toward 4D Trajectory Management in Air Traffic Control: A Study Based on Monte Carlo Simulation and Reachability Analysis," *IEEE Transactions on Control Systems Technology*, vol. 21, no. 5, pp. 1820–1833, Sep. 2013.

[32] EUROCONTROL, "User Manual for the Base of Aircraft Data (BADA) Rev. 3.12," EEC Technical/Scientific No. 14/04/24-44, 2014.

[33] E. Cinquemani, M. Agarwal, D. Chatterjee, and J. Lygeros, "Convexity and convex approximations of discrete-time stochastic control problems with constraints," *Automatica*, vol. 47, no. 9, pp. 2082–2087, 2011.

[34] A. Prékopa, "Stochastic programming, volume 324 of mathematics and its applications," 1995.

[35] G. Calafiore and L. Fagiano, "Robust model predictive control via scenario optimization," *IEEE Transactions on Automatic Control*, vol. 58, no. 1, pp. 219–224, 2013.

[36] "IBM ILOG CPLEX Optimizer," http://www-01.ibm.com/software/commerce/optimization/cplex-optimizer/index.html, 2015.

[37] T. Alamo, R. Tempo, and A. Luque, "On the sample complexity of randomized approaches to the analysis and design under uncertainty," in *2010 American Control Conference*, Baltimore, MD, USA, Jun. 2010, pp. 4671–4676.

[38] T. Alamo, R. Tempo, A. Luque, and D. Ramirez, "Randomized methods for design of uncertain systems: Sample complexity and sequential algorithms," *Automatica*, vol. 52, pp. 160–172, 2015.

[39] G. Schildbach, L. Fagiano, and M. Morari, "Randomized solutions to convex programs with multiple chance constraints," *SIAM Journal on Optimization*, vol. 23, no. 4, pp. 2479–2501, 2013.

[40] A. Domahidi, A. Zgraggen, M. Zeilinger, M. Morari, and C. Jones, "Efficient interior point methods for multistage problems arising in receding horizon control," in *IEEE Conference on Decision and Control*, Maui, HI, USA, Dec. 2012, pp. 668 – 674.

Luca Deori received the laurea triennale cum laude in Control Engineering (2010), the laurea specialistica cum laude in Control Engineering (2012), and the Ph.D. in Information Technology Engineering (2015) from Politecnico di Milano, Italy. In 2016, he was a post-doctoral researcher with the Dipartimento di Elettronica, Informazione e Bioingegneria of the Politecnico di Milano, and also held an academic visitor position at the University of Oxford, UK. His research interests include optimization and control of complex uncertain systems, with application to air traffic control, electric vehicle charging control, and optimal energy management in buildings.

Simone Garatti is an associate professor at the Dipartimento di Elettronica, Informazione e Bioingegneria of the Politecnico di Milano. He received the Laurea degree and the Ph.D. in Information Technology Engineering in 2000 and 2004, respectively, both from the Politecnico di Milano, Milano, Italy. He has been a visiting scholar at the Lund University of Technology, Lund, Sweden, at the University of California San Diego (UCSD), San Diego, CA, USA, and at the Massachusetts Institute of Technology and the Northeastern University, Boston, MA, USA. He is a member of the IEEE Technical Committee on Computational Aspects of Control System Design and of the IFAC Technical Committee on Modeling, Identification and Signal Processing. His research interests include system identification and model quality assessment, identification of interval predictor models, and stochastic and data-based optimization for problems in systems and control.

Maria Prandini received her Ph.D. degree in Information Technology from Università degli Studi di Brescia, Italy, in 1998. She was a postdoctoral researcher at University of California at Berkeley (1998-2000). She held visiting positions at Delft University of Technology (1998), Cambridge University (2000), University of California at Berkeley (2005), and Swiss Federal Institute of Technology Zurich (2006). In 2002, she started as an assistant professor at Politecnico di Milano, Italy, where she is currently a full professor. Her research interests include hybrid systems, stochastic and distributed optimization, constrained control, system verification, with application to air traffic management and energy systems. She was an associate editor of IEEE Transactions on Automatic Control, IEEE Transactions on Control Systems Technology, and Nonlinear Analysis: Hybrid Systems. She was editor for Electronic Publications of the IEEE CSS (2013-15), elected member of the IEEE CSS Board of Governors (2015-17), and CSS Vice-President for Conference Activities (2016-17).